



Toward New Modalities in VEP-Based BCI Applications Using Dynamical Stimuli: Introducing Quasi-Periodic and Chaotic VEP-Based BCI

Zahra Shirzhiyan^{1,2,3}, Ahmadreza Keihani^{2,3}, Morteza Farahi^{2,3}, Elham Shamsi², Mina GolMohammadi³, Amin Mahnam⁴, Mohsen Reza Haidari^{5*} and Amir Homayoun Jafari^{2,3*}

¹ Computational Neuroscience, Institute of Medical Technology, Brandenburg University of Technology Cottbus-Senftenberg, Cottbus, Germany, ² Department of Medical Physics & Biomedical Engineering, School of Medicine, Tehran University of Medical Sciences, Tehran, Iran, ³ Research Center for Biomedical Technologies and Robotics (RCBTR), Tehran University of Medical Sciences, Tehran, Iran, ⁴ Department of Biomedical Engineering, Faculty of Engineering, University of Isfahan, Isfahan, Iran, ⁵ Section of Neuroscience, Department of Neurology, Faculty of Medicine, Baqiyatallah University of Medical Sciences, Tehran, Iran

OPEN ACCESS

Edited by:

Elisa Donati,
ETH Zürich, Switzerland

Reviewed by:

Omid Kavehei,
The University of Sydney, Australia
Eugenie Roudaia,
McMaster University, Canada

*Correspondence:

Mohsen Reza Haidari
drmohsinraza2012@yahoo.com
Amir Homayoun Jafari
h_jafari@tums.ac.ir

Specialty section:

This article was submitted to
Neuromorphic Engineering,
a section of the journal
Frontiers in Neuroscience

Received: 13 February 2020

Accepted: 15 September 2020

Published: 17 November 2020

Citation:

Shirzhiyan Z, Keihani A, Farahi M, Shamsi E, GolMohammadi M, Mahnam A, Haidari MR and Jafari AH (2020) Toward New Modalities in VEP-Based BCI Applications Using Dynamical Stimuli: Introducing Quasi-Periodic and Chaotic VEP-Based BCI. *Front. Neurosci.* 14:534619. doi: 10.3389/fnins.2020.534619

Visual evoked potentials (VEPs) to periodic stimuli are commonly used in brain computer interfaces for their favorable properties such as high target identification accuracy, less training time, and low surrounding target interference. Conventional periodic stimuli can lead to subjective visual fatigue due to continuous and high contrast stimulation. In this study, we compared quasi-periodic and chaotic complex stimuli to common periodic stimuli for use with VEP-based brain computer interfaces (BCIs). Canonical correlation analysis (CCA) and coherence methods were used to evaluate the performance of the three stimulus groups. Subjective fatigue caused by the presented stimuli was evaluated by the Visual Analogue Scale (VAS). Using CCA with the M2 template approach, target identification accuracy was highest for the chaotic stimuli ($M = 86.8$, $SE = 1.8$) compared to the quasi-periodic ($M = 78.1$, $SE = 2.6$, $p = 0.008$) and periodic ($M = 64.3$, $SE = 1.9$, $p = 0.0001$) stimulus groups. The evaluation of fatigue rates revealed that the chaotic stimuli caused less fatigue compared to the quasi-periodic ($p = 0.001$) and periodic ($p = 0.0001$) stimulus groups. In addition, the quasi-periodic stimuli led to lower fatigue rates compared to the periodic stimuli ($p = 0.011$). We conclude that the target identification results were better for the chaotic group compared to the other two stimulus groups with CCA. In addition, the chaotic stimuli led to a less subjective visual fatigue compared to the periodic and quasi-periodic stimuli and can be suitable for designing new comfortable VEP-based BCIs.

Keywords: VEP-based BCI, chaotic stimuli, quasi-periodic stimuli, CCA, coherence

INTRODUCTION

Electroencephalogram (EEG) is commonly used for EEG-based brain computer interfaces (BCIs) as a non-invasive and low-cost method for measuring the brain neural activities (Wolpaw et al., 2002; Lebedev and Nicolelis, 2006). BCI applications employing EEG use visual evoked potentials (VEPs) (Middendorf et al., 2000; Müller-Putz et al., 2005; Lee et al., 2006, 2008;

Wang et al., 2006; Wang Y. et al., 2017; Martinez et al., 2007; Allison et al., 2008; Guo et al., 2008; Chen et al., 2015; Xie et al., 2017, 2018), which are responses of the visual system to visual stimuli. Various types of visual stimuli, such as flickering LED, can be decoded from the EEG activity of the visual cortex and used for diverse BCI applications (Takano et al., 2009; Lee et al., 2011; Gao et al., 2014; Kapgate and Kalbande, 2015).

In VEP-based BCIs, the target stimuli are identified by decoding all the gazed stimuli. The stimuli are required to be orthogonal or almost orthogonal in time-, frequency-, or code-based BCIs (Bin et al., 2009a). The oddball paradigm is an example of time-based BCIs, whereby the target stimuli are presented at different times and evoke event-related potentials (ERPs) like the P300 (Jin et al., 2005; Lee et al., 2008; McCane et al., 2015). Frequency-based BCIs may use visual stimuli that are modulated in time according to a sine wave with different temporal frequencies, which also evoke EEG responses at the same frequencies and their harmonics (Middendorf et al., 2000; Müller-Putz et al., 2005; Wang et al., 2006). Orthogonal visual stimuli in code-based BCIs are generated by random codes such as *m*-sequences, whereby different shifts of a modulating code have been used to evoke code-modulated VEPs (c-VEPs) (Nakanishi et al., 2014; Riechmann et al., 2016; Wei et al., 2016, 2018; Spüler, 2017; Liu et al., 2018; Shirzhiyan et al., 2019).

Due to their high decoding accuracy, external stimuli such as periodic flickers are commonly used in VEP-based BCIs evoking steady-state visual evoked potentials (SSVEPs) (Vialatte et al., 2010; Keihani et al., 2018). In SSVEP-based BCIs, the stimulus comprises a constant frequency that varies from low to high (1–100 Hz), which then leads to specific EEG responses that correlate with the stimulus frequency (Vialatte et al., 2010). Therefore, the gazed target stimuli could be identified from their EEG responses. However, among different frequency sets, the lower (1–12 Hz) and medium (13–16 Hz) ones lead to high subjective discomfort, fatigue, and possible epileptic seizures (Volosyak et al., 2011). Various dynamical approaches have also been used for improving SSVEP-based BCIs, such as dynamic stopping methods and the detection of SSVEP responses for higher information transfer rate (ITR) SSVEP-based BCIs (Yin et al., 2014; Jiang et al., 2018).

Visual stimuli have diverse dynamical patterns such as periodic, quasi-periodic, and chaotic. Biological systems also exhibit these dynamical behaviors (Attinger et al., 1966; Petrov et al., 1997; Suzuki et al., 2016) including non-oscillatory chaotic behavior, which is more complex than quasi-periodic oscillation (Camazine et al., 2003; Saha and Galic, 2018; Strogatz, 2018). Neuronal systems exhibit both complex oscillatory behavior (Llinás, 1988; Zhanabaev and Kozhagulov, 2013; Zhanabaev et al., 2016; Feng et al., 2017) as well as the non-oscillatory chaotic behavior that is seen in neurons (Aihara et al., 1984; Hong, 2011; Lv et al., 2016; Ma and Tang, 2017) and networks (Aihara, 1989; Freeman, 1992; Potapov and Ali, 2000; Rössert et al., 2015; Nobukawa and Nishimura, 2016) due to various underlying mechanisms (Hoebeek et al., 2010; Ishikawa et al., 2015). Stimuli with dynamical patterns such as chaotic behaviors are thus expected to be more in harmony with the visual system.

Natural visual stimuli rarely flicker at a constant rate, but rather exhibit more complex dynamics with quasi-periodic temporal characteristics (Kayser et al., 2003; Butts et al., 2007;

Mazzoni et al., 2011). Natural visual stimuli are efficiently encoded by the visual system which is capable of processing and detecting information from complex natural environments (Blake and Lee, 2005; Mazzoni et al., 2011). These visual stimuli have similar spatial and temporal patterns resembling the $1/f$ amplitude spectrum, features that are encoded more efficiently by the retina and other components of the visual system (Atick and Redlich, 1992; Yoshimoto et al., 2017). In addition, chaotic patterns also follow the $1/f$ spectrum observed in natural scenes and phenomena (Relano et al., 2002; Molina et al., 2010). Quasi-periodic visual stimuli can generate phase-locked responses (Keitel et al., 2017; Obleser et al., 2017; Haegens and Golumbic, 2018) and also evoke responses with independent dynamics that correlate with their corresponding stimuli (Keitel et al., 2017). Temporal dynamics of the presented visual stimuli leads to adjustment of the visual system based on its inherent characteristics (Lasley and Cohn, 1981; Correa and Nobre, 2008). For these reasons, it is possible to assume that complex stimuli with dynamical temporal patterns such as quasi-periodic and chaotic may generate correlated responses which may lead to greater visual comfort for the viewer compared to the periodic stimuli.

One of the important issues in VEP-based BCI applications is the subjective visual fatigue caused by the flickering stimuli (Volosyak et al., 2011; Chang et al., 2014; Won et al., 2015). Periodic stimuli generating SSVEPs, due to their high contrast flashes, are not comfortable and can lead to subjective visual fatigue (Kardan et al., 2015; Xie et al., 2016). These periodic patterns may also lead to migraine headache (DeTommaso et al., 1999) or even epileptic seizures (Fisher et al., 2005). Studies have used various methods including the use of high-frequency stimuli rather than lower frequencies (Allison et al., 2010; Sakurada et al., 2015; Ajami et al., 2018), polychromatic stimuli (Chien et al., 2017), motion Newton's rings and motion checkerboards (Xie et al., 2012, 2017; Yan et al., 2017; Han et al., 2018), and rhythmic pattern stimuli (Keihani et al., 2018) to minimize the subjective visual fatigue, which still remains an important problem in VEP-based BCI applications.

Utilization of visual stimuli with quasi-periodic and chaotic patterns that are closer to natural scenes in BCI applications requires further research. In our previous study, we used chaotic and pseudo-random *m*-sequence binary codes and found that chaotic codes lead to comparatively less fatigue (Shirzhiyan et al., 2019). In this study, we introduce a new kind of visual stimuli with quasi-periodic and chaotic characteristics to evoke distinct visual potentials in normal subjects for their possible application in VEP-based BCIs. For comparison, we used periodic stimuli commonly employed in SSVEP-based BCI applications and also compared subjective visual fatigue caused by these three groups of stimuli.

MATERIALS AND METHODS

In this study, first of all, the stimulus groups were designed and proper setup for the experiment was prepared. The data recording step started with EEG and behavioral data (fatigue data) recording from normal subjects. After preprocessing of

the EEG data, the data analysis was done to decode the presented stimuli from their corresponding data using canonical correlation analysis (CCA) and coherence analysis methods. These two methods calculate the similarity of templates with EEG signals where the stimuli could be considered as templates (template generation approach M1) or obtained from a training dataset (template generation approach M2). Finally, the target identification results using the above-mentioned methods and the fatigue data were analyzed separately. The flowchart of this study is presented in **Figure 1**.

Study Participants

Our study was announced in the faculties of medicine and biomedical engineering *via* notice boards as well as in students' social media groups. Forty-eight volunteers were initially enrolled based on the inclusion criteria (normal or corrected vision with no history of head trauma and without current use of drugs). All subjects were informed about the study aims and procedure of signal recording and were allowed to leave the experiment at any point if they wished. Thirty-eight subjects participated in all the sessions (18 females), aged 20–33 years old (23.01 ± 4.32). The remaining 10 subjects did not participate in all the sessions or left the session due to urgent work, and so their data were excluded from the study. Written informed consent was signed by the participants before joining the study in accordance with the Declaration of Helsinki. The study was approved by the Office of Research Review Board and the Research Ethics Committee of the Tehran University of Medical Sciences, with LREC protocol number IR.TUMS.REC.1394.2110.

Stimuli

We used visual stimuli consisting of modulating the brightness of a red color LED measuring 4 cm × 4 cm according to three different temporal patterns: periodic, quasi-periodic, or chaotic. Each of these three categories had four different target stimuli that had their orthogonal characteristics. All the stimuli were generated using MATLAB software (Release 2016b, The MathWorks, 193 Inc., Natick, MA, United States).

Periodic Stimuli

For generating the periodic stimuli, we used four sine waves at the target frequencies of $f_1 - f_4$ (20, 25, 35, and 40 Hz), as shown in Equation 1 and schematically illustrated in **Figure 2A**. It can be seen that the simple periodic stimulus group ($P_1 - P_4$) had constant frequencies and that their spectrum was sparse in the frequency domain representation.

$$P_i = \sin(2\pi f_i t) \cdot t = 0 : 6 \text{ sec. } f = [20 \text{ Hz} \cdot 25 \text{ Hz} \cdot 35 \text{ Hz} \cdot 40 \text{ Hz}] \quad (1)$$

Quasi-Periodic Stimuli

A sine-circle map was used to generate four quasi-periodic stimuli (Essl, 2006). Equation 2 models the sinusoidal oscillators that were perturbed by non-linear function.

$$\theta_{n+1} = \theta_n + \Omega - K/2\pi \sin(2\pi\theta_n) \quad (2)$$

where Ω is the frequency ratio and K is the coupling length of non-linear perturbation.

If the frequency ratio Ω is a rational number (p/q) with p and $q \in N$ (natural numbers), the map shows periodic behavior. For irrational numbers of Ω and appropriate parameters of K , the behavior of the sine-circle map is called quasi-periodic oscillation (Essl, 2006).

Quasi-periodic stimuli were generated using a sine-circle map by considering the parameter $K = 0.5$ and then Ω were selected as irrational numbers ($(\sqrt{5} - 1)/2$, $\sqrt{3} - 1$, $\sqrt{3}/2$, and $\sqrt{2}/9$), where the sine-circle map showed quasi-periodic behaviors. These parameters were used to generate quasi-periodic stimuli Q_1 , Q_2 , Q_3 , and Q_4 . After that, the generated sequences from the sine-circle maps were considered as a time series with a sampling frequency of 90 Hz. Thus, each sample of the sequences was applied for a duration of 1/90 ms. The waveform and spectrum of the quasi-periodic stimuli are shown in **Figure 2B**. The waveform and spectrum of the quasi-periodic stimuli were more complex compared to the periodic stimulus group.

Chaotic Stimulus Group

For generating chaotic stimuli, we used a logistic map which is a one-dimensional map capable of generating chaotic signals with low cross-interferences. This map is seen in most of the natural phenomena and population growth of biological species (Costantino et al., 1997), as defined in Equation 3.

$$x(i+1) = A x(i) (1 - x(i)) \quad (3)$$

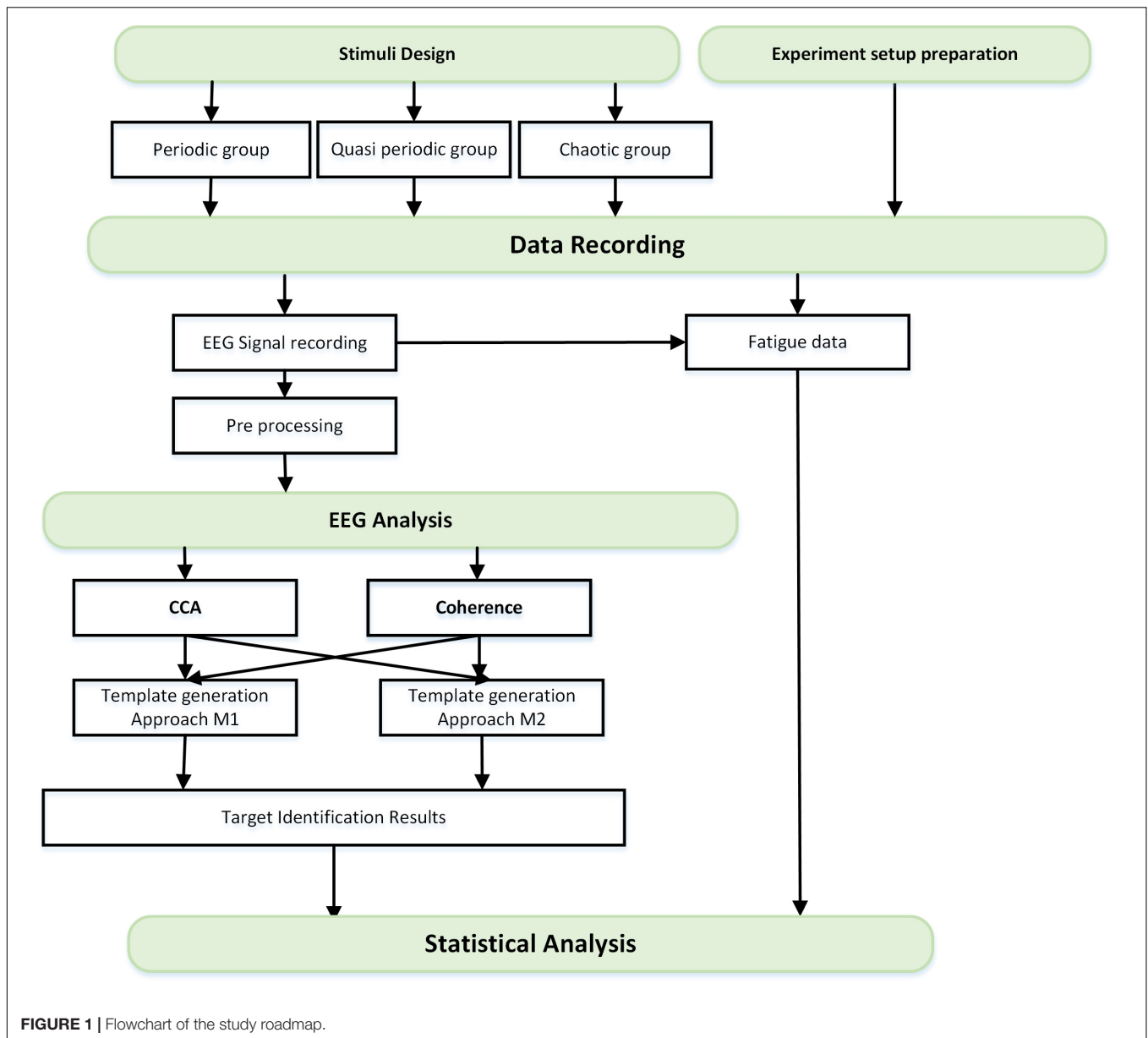
where x is in the interval of $[0 \ 1]$ and indicates the ratio of an existing population to the maximum possible population, $x(0)$ as the initial value of x , and A is the rate of reproduction and starvation that is in the interval of $[0 \ 4]$. This simple map could generate chaotic dynamics in some values of parameter A generally between 3.5 and 4 (May, 1976). Parameter A was chosen in a way that the logistic map exhibited chaotic behaviors for generating four chaotic sequences and were then presented at the rate of 90 Hz as $A = 3.982$, 3.885 , 3.987 , and 4 , respectively. In this way, four different chaotic stimuli, Ch_1 , Ch_2 , Ch_3 , and Ch_4 , were generated by the logistic map.

Figure 2C shows the waveforms of four chaotic stimuli with their amplitude spectra.

The dotted black curved line in the amplitude spectra plots shows the $1/f$ line, where f is the frequency vector (horizontal axis). It can be seen that the amplitude spectra of the stimuli in the chaotic group are closer to the $1/f$ spectrum line compared to the quasi-periodic and periodic stimulus groups. Please note that for better illustration, only 1 s of the total 6 s duration of every stimulus is shown in the plot.

Auto- and Cross-Correlation Function of Target Stimuli

The auto- and cross-correlation functions of the periodic, quasi-periodic, and chaotic stimulus groups were calculated to investigate their individual orthogonal characteristics. This was done to verify overlapping characteristics in order to avoid interference between the target stimuli. The auto- and cross-correlation functions of the periodic, quasi-periodic, and chaotic



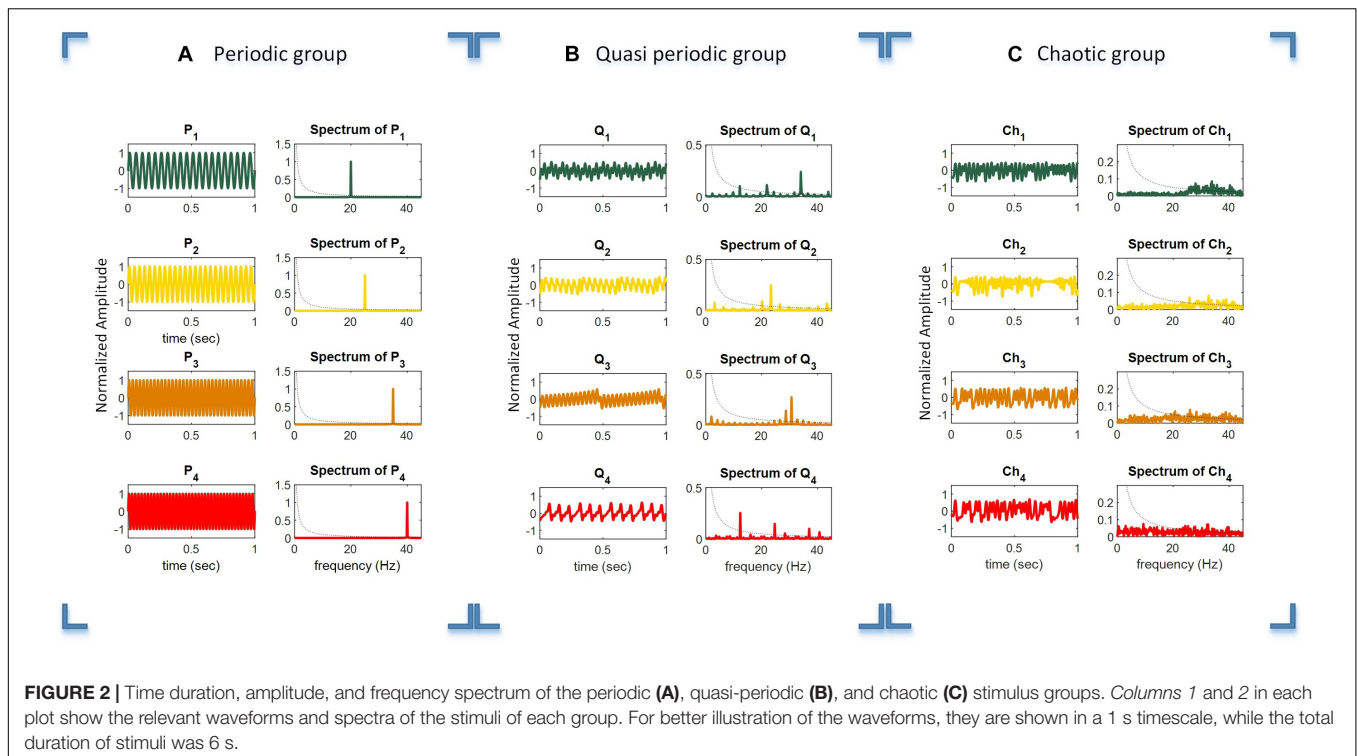
groups are presented in **Figures 3A–C**, respectively. It is obvious that the auto-correlation function of each target stimulus group is high, while within-group cross-correlations of stimuli with others is comparatively low.

Stimulus Presentation Paradigm

All the subjects were presented with periodic, quasi-periodic, and chaotic stimuli in a single lab visit. They were presented with each of the periodic ($P_1 - P_4$), quasi-periodic ($Q_1 - Q_4$), and chaotic ($Ch_1 - Ch_4$) stimuli as 12 different sessions. The total duration of each session (for each stimulus) was 90 s consisting of 10 trials. In each trial (6 s duration), the same stimulus was presented to the subject with a 2 s rest time in between the trials. An initial rest of 10 s was included in each session. After each session (90 s), the subjective fatigue was evaluated (see below). The maximum

duration of a whole stimulus presentation paradigm including rest time was approximately 30 min. The stimulus presentation paradigm is shown in **Figure 4**.

The subjects were informed before the experiment that they will be asked to evaluate their own visual fatigue by considering the amount of tiredness and discomfort caused by gazing at the stimuli. They were asked to grade their visual fatigue level by choosing a number between 0 for no fatigue and 10 for the highest fatigue level. After each session (90 s), the subjects were asked to self-report the level of visual fatigue caused by stimulation. Their fatigue rate was recorded and they were asked for permission to start the next session. The order of presentation of stimuli in all groups was randomly distributed for all subjects to avoid possible bias in subjective visual fatigue caused by the order of presentation.



Fatigue Evaluation Process

The level of subjective visual fatigue was measured using graded values of the Visual Analogue Scale (VAS), which is suitable for grading continuous phenomena (Aitken, 1969). The VAS is a subjective estimation method for quantifying a feeling and attitude which is hard to estimate directly (Gift, 1989; Grant et al., 1999; Crichton, 2001; Tseng et al., 2010; Klimek et al., 2017). This scale is mostly used in clinical research for measuring the intensity of various symptoms (Paul-Dauphin et al., 1999) such as pain (Bijur et al., 2001). It is commonly used in BCI applications for the evaluation of a patient's motivation and mood (Holz et al., 2013), the level of subjective fatigue (Guger et al., 2013; Käthner et al., 2014), pain (Choi, 2017), discomfort (Verwulgen et al., 2018), and control ability (Chumerin et al., 2012).

Signal Recording Setup

The EEG signals were recorded using g.USB Amp with a sampling rate of 1,200 Hz. Four active g.Ladybird electrodes were placed at Oz, O1, O2, and Pz positions on the scalp of the subjects where the visual evoked potentials have maximum amplitude (Bin et al., 2011; Aminaka et al., 2015). Fpz and right earlobe were used as the ground and reference electrodes, respectively. An online bandpass filter with cutoff frequencies of 0.05 and 120 Hz was applied.

The generated stimuli were applied to a custom-made digital-to-analog converter (DAC) board as a stimulus presenter box (shown in **Supplementary Figure 1**) for driving an LED. The LED was placed at a distance of 70 cm from the subject. The trigger output of g.USB Amp (start time of EEG recording) and the output of a Texas Instruments optical sensor (visual stimuli)

were sent to National Instruments (NI) DAQ. Details of the signal recording setup are reported in our previous studies (Keihani et al., 2018; Shirzhiyan et al., 2019).

Data Processing

The signal analysis procedure was carried out for the recorded responses for each stimulus group (periodic, quasi-periodic, and chaotic) (**Supplementary Figure 2**) separately to compare the results of the three different groups. Tenfold cross-validation was used as our validation method. In this method, nine-tenths of the trials were used as the training data and one-tenth was used as the testing data. The training data was used for template generation and the testing data was used for target identification.

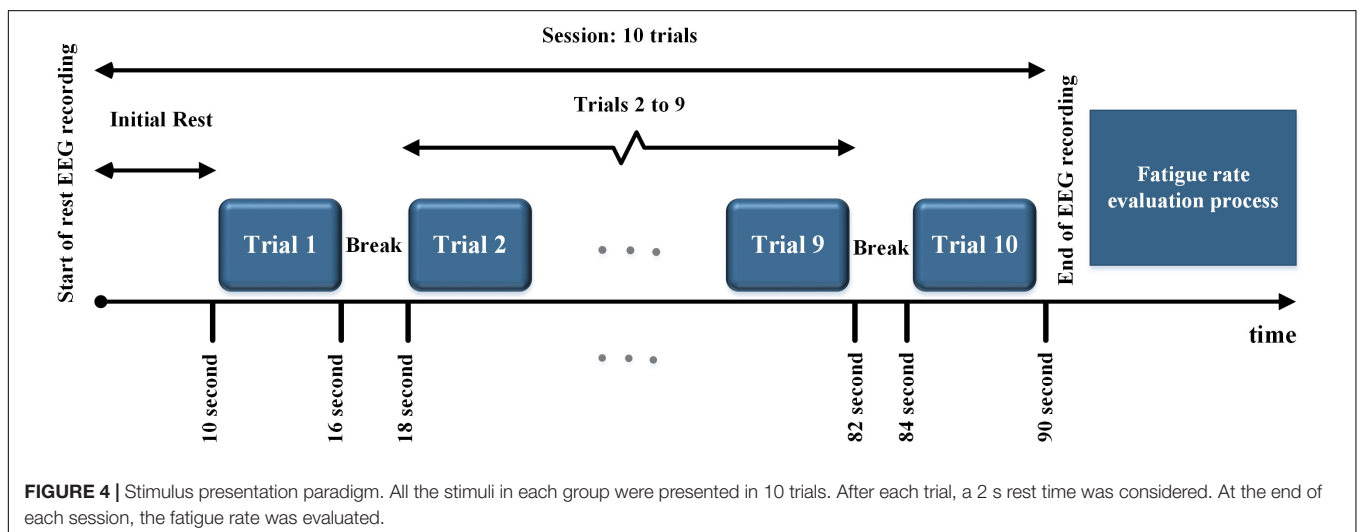
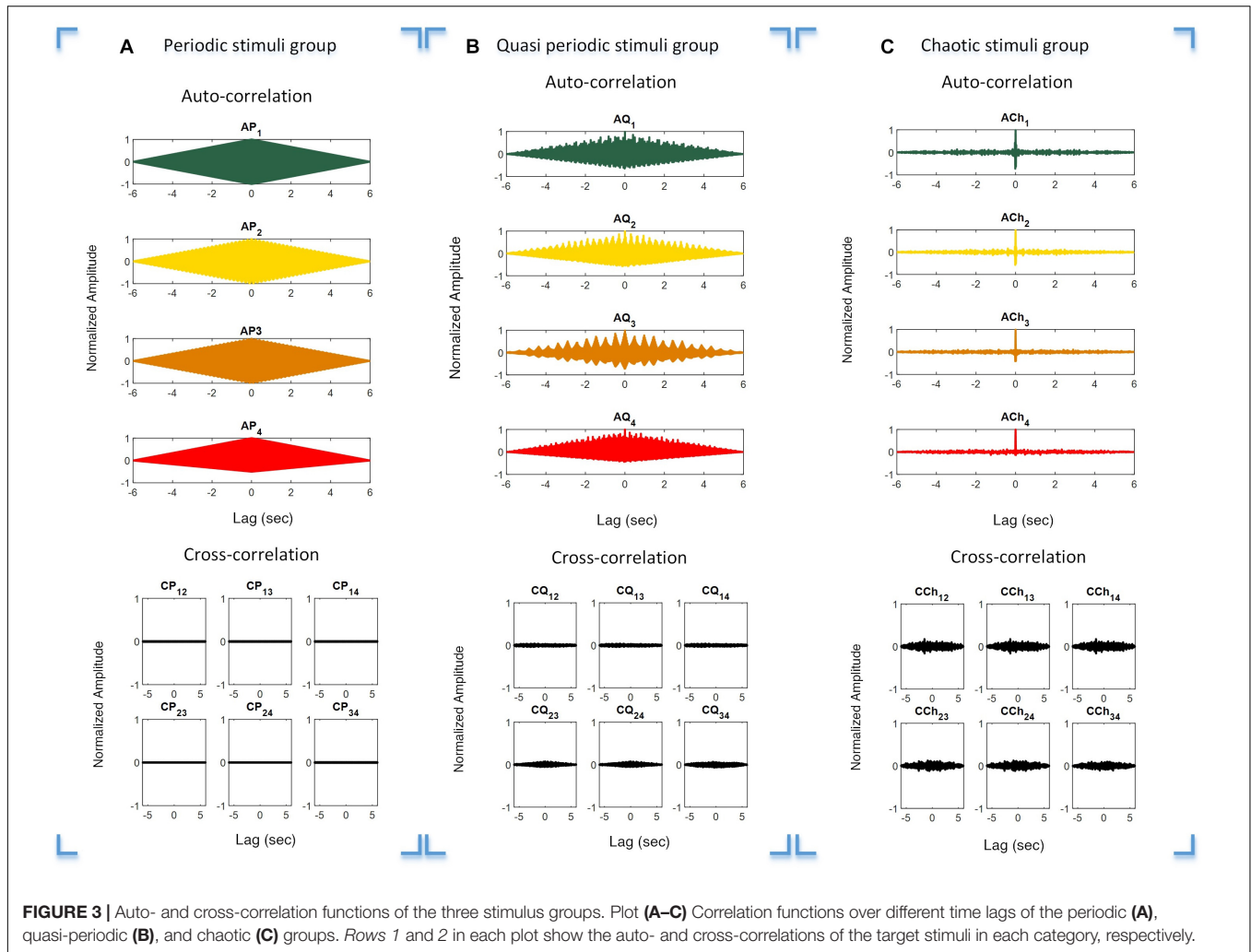
Preprocessing

The recorded trigger from g.USB Amp and sensor output and the presented stimuli in NI DAQ were used for the detection of the beginning of each trial and then each trial EEG data was extracted. A zero-phase eighth-order band pass filter with cutoff frequencies of 1 and 50 Hz was applied for all the trials.

Processing (CCA and Coherence Analysis)

To analyze the EEG data, we used two methods that are commonly employed in BCI studies: CCA and coherence analysis (Zhang et al., 2013, 2014; Vaid et al., 2015). These methods measure the amount of correlation in the time and frequency domains, respectively.

Canonical correlation analysis is a multivariable data analysis method that measures the underlying time domain correlation between two multidimensional signals and attempts to reveal a linear time domain correlation by maximizing the correlation



of the two signals (Lin et al., 2006). CCA has been successfully used in target identification and in the analysis of visual evoked potentials (Lin et al., 2006; Bin et al., 2009b, 2011). Equation

4 defines the CCA coefficient of variables x and y , where $E(x^t y)$ stand for the covariance of x and y and $E(x^t x)$ and $E(y^t y)$ represent the variance of x and y , respectively. This

method finds the canonical correlation vectors W_x and W_y for two multidimensional variables, x and y , by maximizing their canonical covariants.

$$\text{Max}_{w_x, w_y} \rho(x, y) = \frac{E(x^t y)}{\sqrt{E(x^t x) E(y^t y)}} \quad (4)$$

Coherence analysis has been used to investigate the synchronization process of brain regions (Nunez et al., 1997; Lachaux et al., 1999; La Rocca et al., 2014). In addition, it has been used as a feature extraction and target identification method in BCI applications (Gysels and Celka, 2004; Krusienski et al., 2012; Liew et al., 2015). The coherence of two signals is sometimes called magnitude-squared coherence, as shown by Equation 5 which defines the amount of coherence of two signals at a specific frequency.

$$C_{xy}(f) = \frac{|S_{xy}(f)|^2}{S_{xx}(f) S_{yy}(f)} \quad (5)$$

where S_{xx} and S_{yy} are the power spectral densities of variables x and y , respectively, and $S_{xy}(f)$ is the cross power spectral density between x and y (Sanei and Chambers, 2007).

In this study, variable x is the template and y is the EEG signal. In BCI studies, it is common to use either the presented stimuli or the average EEG signal of the training session trials to generate the template. Therefore, in this study, we used two approaches for generating templates. In the first approach (M1), the stimuli were used as templates, while in the second approach (M2), we attempted to extract templates from the training dataset.

Template Generation

Templates were generated by using the two aforementioned approaches as described below.

Approach 1 (M1): using the presented stimuli as templates

The target stimuli were resampled to the sampling frequency of the EEG responses (1,200 Hz) and zero-padded the resampled target stimulus i by lag time D_i . The lag time D_i represents the systematic lag for the presented stimuli and was calculated by cross-correlating the target stimuli with the grand averaged EEG responses and determining the time lag that yielded the maximum cross-correlation values.

This step was not important for coherence analysis because the magnitude-squared coherence was not sensitive to the time lag between templates (stimuli) and responses, while the CCA coefficients were maximum where the lag was considered.

Approach 2 (M2): generating templates using the training dataset

In VEP-based BCI studies, it is also common to create templates using the EEG signals from a subset of the data (i.e., a training dataset) instead of the stimulus waveform itself, as this approach allows capturing information related to the non-linear processing of the system. Given that we had access to the training dataset, we used this approach to generate templates by EEG data from the training dataset.

This approach included extracting the EEG responses from r trials in the training set, $X_{\text{Train}_i}^{r \times m \times n}$, and averaging over r trials to generate the template for stimulus i , $T_i^{m \times n}$, where m is the number of channels and n is the number of samples per trial.

Target Identification

After generating templates separately for the targets in each group, the CCA coefficient and coherence were calculated by Equations 4 and 5, where T was considered as variable x and the EEG response was considered as variable y . For template generation using the M1 approach, all the trials were separately considered as testing trials, while 10-fold cross-validation was considered for template generation using the M2 approach. Here, ninefold of the dataset was considered as the training dataset and the one remaining fold was considered as the testing trial. Therefore, all the trials were tested once. The details of both the approaches of target identification are given below.

For the CCA method:

- (1) Extraction of testing trials $X_{\text{Test}}^{m \times n}$, where m and n are the channel numbers and samples in a trial, respectively.
- (2) Calculation of the CCA coefficient of templates T_i and $X_{\text{Test}}^{m \times n}$ as vector $P_i^{1 \times m}$.
- (3) Calculation of the mean value of $P_i^{1 \times m}$ to create the feature vector.
- (4) Selection of the maximum value of feature vector.

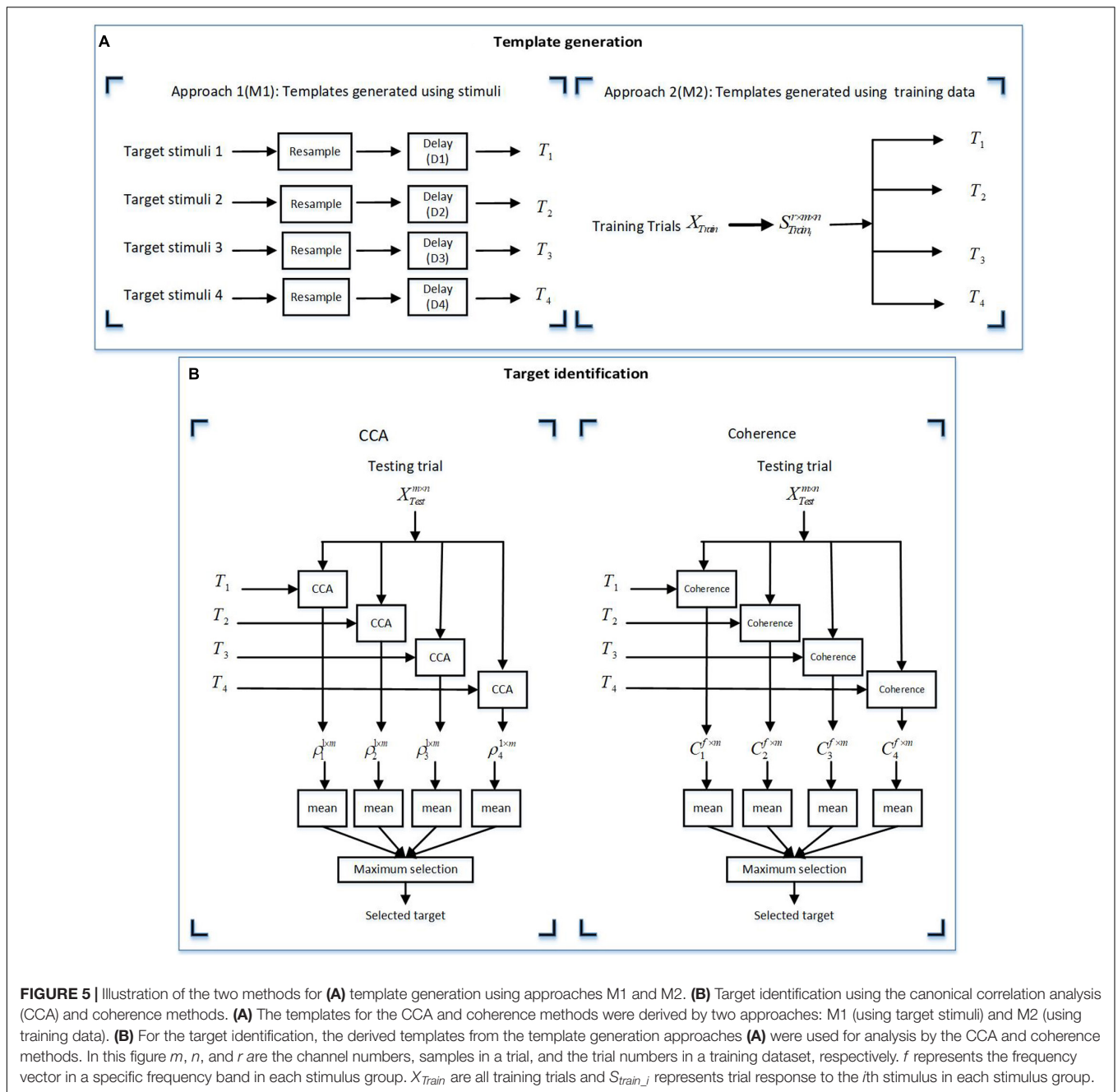
For the coherence method:

- (1) Extraction of testing trials $X_{\text{Test}}^{m \times n}$, where m and n are the channel numbers and samples in a trial, respectively.
- (2) Calculation of the coherence function of templates T_i and $X_{\text{Test}}^{m \times n}$ for obtaining the vector $C_i(f)$.
- (3) Extraction of the coherence coefficient from vector of $C_i(f)$ in the target frequencies or a specific frequency band.
 - (a) Periodic group: the target frequencies in the periodic group were the target frequencies of the presented stimuli as shown in **Figure 2A**.
 - (b) Quasi-periodic group: the dominant frequencies of the presented stimuli are shown in the spectra of stimuli in **Figure 2B**.
 - (c) Chaotic group: the total frequency band of the chaotic stimuli as shown in **Figure 2C**.
- (4) Calculation of the mean value of $C_i^{m \times f}$ to create the feature vector.
- (5) Selection of the maximum value of the feature vector.

Figure 5 schematically shows the template generation and target identification processes.

Statistical Analysis

Statistical analysis was done with SPSS software (version 16.0, SPSS Inc., IBM Corp., Chicago, released 2011) for comparing the analysis methods and also for evaluating the subjective visual fatigue rate between the three groups of stimuli (periodic, quasi-periodic, and chaotic).



Statistical Analysis of Accuracies

Three-way repeated measures ANOVA was used to test the effects of three factors—methods (CCA and coherence), approaches (M1 and M2), and stimulus groups (periodic, quasi-periodic, and chaotic)—with assumed sphericity (significance level $\alpha = 0.05$). Confidence intervals were adjusted by Bonferroni correction for pairwise comparisons.

Statistical Analysis of Fatigue Rates

Within-group analysis of fatigue rates

To compare the VAS scores across stimuli within each stimulus type (periodic, quasi-periodic, and chaotic), the

Friedman test (significance level $\alpha = 0.05$) was used. Then, the scores for each pair of stimuli were compared using the Wilcoxon signed-rank test, with a Bonferroni-corrected alpha set to 0.008.

Between-group analysis of subjective visual fatigue rates

For comparison of the subjective visual fatigue caused by the periodic, quasi-periodic, and chaotic groups, the VAS scores of each group were averaged for the four sessions for each stimulus type for each subject and were then compared using the Friedman test (significance level $\alpha = 0.05$). The Wilcoxon signed-rank test with Bonferroni correction was

used for the comparison of each pair while α was set at 0.0168.

RESULTS

Accuracy Analysis Results

The descriptive statistics of all accuracies of the three stimulus groups (periodic, quasi-periodic, and chaotic) obtained from two different methods (CCA and coherence) and template generation approaches (M1 and M2) are reported in **Table 1**, and **Figure 6** shows the estimated marginal means plots of accuracies.

The 2 (analysis method) \times 2 (template approach) \times 3 (stimulus group) ANOVA on target identification accuracy

revealed significant main effects of analysis method [$F(1,37) = 60.253, p = 0.0001, \eta_p^2 = 0.620$] and template approach [$F(1,37) = 28.56, p = 0.0001, \eta_p^2 = 0.435$], but not stimulus group [$F(1,37) = 1.143, p = 0.324, \eta_p^2 = 0.030$], with overall higher accuracy for the CCA method relative to coherence and higher accuracy for the M1 template approach relative to M2.

However, these effects were qualified by significant two-way interactions between analysis method and stimulus group [$F(2,74) = 47.0009, p = 0.0001, \eta_p^2 = 0.56$] and template approach and stimulus group [$F(2,74) = 8.776, p = 0.0001, \eta_p^2 = 0.192$]. The interaction between analysis method and template approach was not significant [$F(1,37) = 3.695, p = 0.062, \eta_p^2 = 0.091$]. Finally, the three-way interaction was significant [$F(2,74) = 35.74, p = 0.0001, \eta_p^2 = 0.491$]. To decompose the three-way interaction, we

TABLE 1 | Descriptive statistics of all accuracies obtained by two methods (CCA and coherence analysis) with two template generation approaches (M1 and M2) in three different stimulus groups.

Method	Approach	Stimulus group	Mean (%)	Standard error (%)	95% Confidence interval	
					Lower bound (%)	Upper bound (%)
CCA	M1	P	79.5	2.4	74.8	84.3
		Q	73.2	2.3	68.5	77.9
		Ch	85.1	2.2	80.6	89.7
	M2	P	64.3	1.9	60.5	68.2
		Q	78.1	2.6	72.8	83.4
		Ch	86.8	1.8	83.1	90.4
Coherence	M1	P	75.0	2.2	70.5	79.5
		Q	70.5	2.7	65.1	76.0
		Ch	70.2	2.7	64.7	75.7
	M2	P	74.5	2.5	69.5	79.6
		Q	65.7	2.7	60.1	71.2
		Ch	58.8	3.0	52.7	64.8

CCA, canonical correlation analysis; M1, using target stimuli; M2, using training data; P, periodic; Q, quasi-periodic; Ch, chaotic.

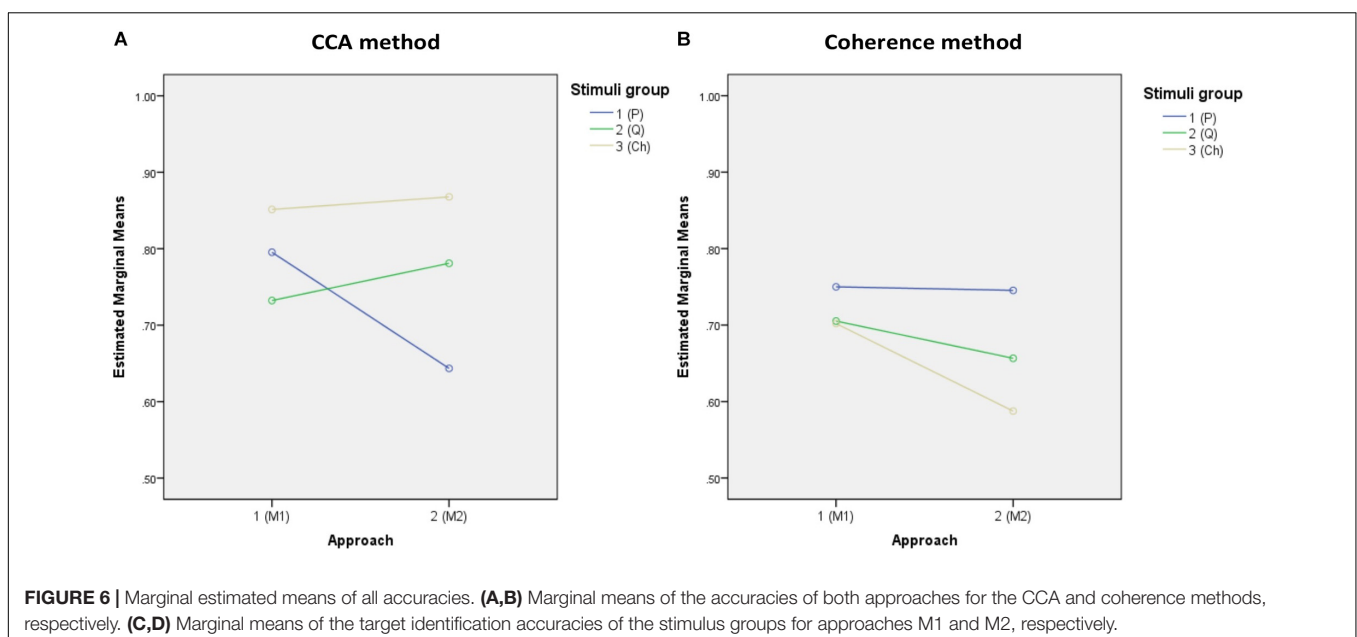


FIGURE 6 | Marginal estimated means of all accuracies. (A,B) Marginal means of the accuracies of both approaches for the CCA and coherence methods, respectively. (C,D) Marginal means of the target identification accuracies of the stimulus groups for approaches M1 and M2, respectively.

examined the effects of stimulus group for each analysis method and template separately and conducted pairwise comparisons between the stimuli groups.

For CCA and template approach M1, accuracy was higher for the chaotic stimuli ($M = 85.1$, $SE = 2.2$) than for periodic ($M = 79.5$, $SE = 2.4$, $p = 0.0001$) and quasi-periodic ($M = 73.2$, $SE = 2.3$, $p = 0.008$), with quasi-periodic also being lower than periodic ($p = 0.0001$). With template approach M2, CCA accuracy was again higher for the chaotic group ($M = 86.8$, $SE = 1.8$) compared to the other two groups, the accuracy now being better for the quasi-periodic ($M = 78.1$, $SE = 2.6$) than for the periodic stimuli ($p = 0.0001$) (Figure 6A).

For coherence analysis, using M1 template approach, multiple comparison with $\alpha = 0.0168$ did not show significant differences between the periodic ($M = 75.0$, $SE = 2.2$), chaotic ($M = 70.2$, $SE = 2.7$), and quasi-periodic ($M = 70.5$, $SE = 2$, $p > 0.0168$) stimulus groups. Using M2 template approach, the periodic group ($M = 74.5$, $SE = 2.5$) showed higher accuracy than did the chaotic group ($M = 58.8$, $SE = 3$, $p = 0.001$), and the quasi-periodic group ($M = 65.5$, $SE = 2.7$) did not significantly differ from the other groups ($p > 0.02$) (Figure 6B).

VAS Scores Analysis Results

The subjective fatigue VAS scores for the four stimuli within each stimulus group are shown in Figure 7 and the averaged scores for each stimulus group are shown in Figure 8.

Results of Within-Group Analysis of the Periodic Group

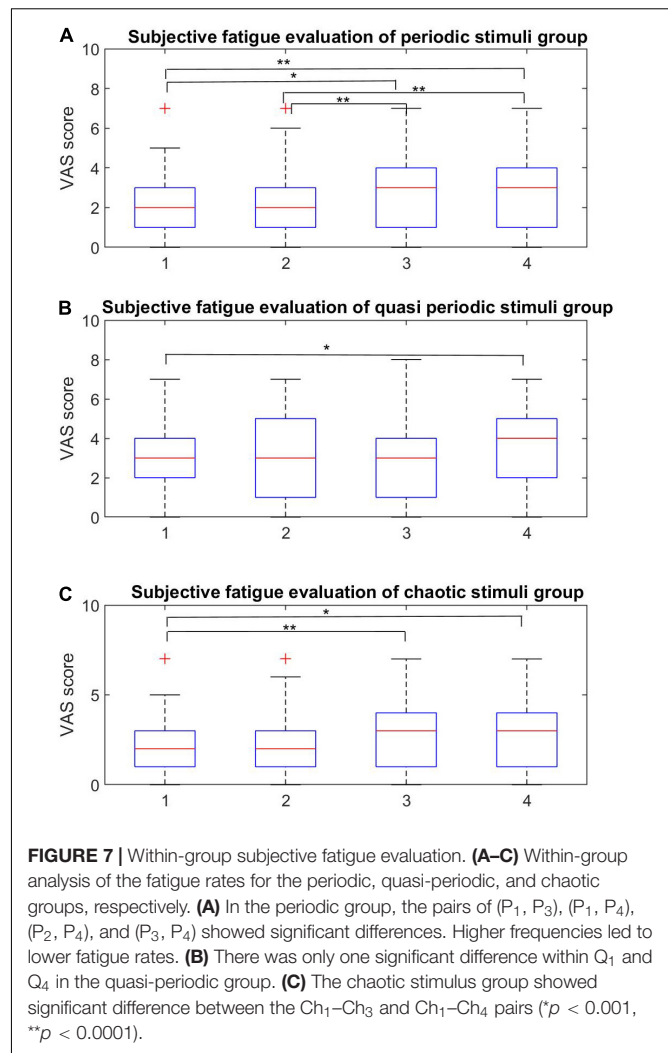
The Friedman test showed significant differences in the VAS scores across stimuli in the periodic group [$\chi^2(3) = 37.857$, $p = 0.0001$]. Participants reported on average highest subjective fatigue scores for P₁ (20 Hz) ($M = 4.92$, $SE = 0.38$) and P₂ (25 Hz) ($M = 4.5$, $SE = 0.30$), which did not differ from each other ($Z = 1.99$, $p = 0.046$). The scores for P₃ (30 Hz) were significantly lower ($M = 3.2$, $SE = 0.22$) than for P₂ ($p < 0.001$), and P₄ had the lowest scores ($M = 2.71$, $SE = 0.28$).

Results of Within-Group Analysis of the Quasi-Periodic Group

The Friedman test showed significant differences among the VAS scores of stimuli in the quasi-periodic group [$\chi^2(3) = 14.848$, $p = 0.002$]. Q₄ ($M = 3.65$, $SE = 0.32$) caused relatively higher fatigue scores compared to Q₁ ($M = 3.08$, $SE = 0.30$, $Z = 2.85$, $p = 0.004$) in the pairwise comparison of within-group quasi-periodic stimuli. Q₂ ($M = 3.13$, $SE = 0.30$) and Q₃ ($M = 3.05$, $SE = 0.326$) did not differ significantly from the others.

Results of Within-Group Analysis of the Chaotic Group

The Friedman test showed significant differences in the VAS scores for the stimuli in the chaotic group [$\chi^2(3) = 20.125$, $p = 0.0001$]. Ch₁ ($M = 2.02$, $SE = 0.28$) had lower fatigue scores compared to Ch₃ ($M = 2.78$, $SE = 0.31$, $Z = 3.53$, $p = 0.0001$), and Ch₄ ($M = 2.84$, $SE = 0.30$, $Z = 2.79$, $p = 0.005$). Ch₂ ($M = 1.78$, $SE = 0.28$) did not differ from Ch₁ and Ch₄.



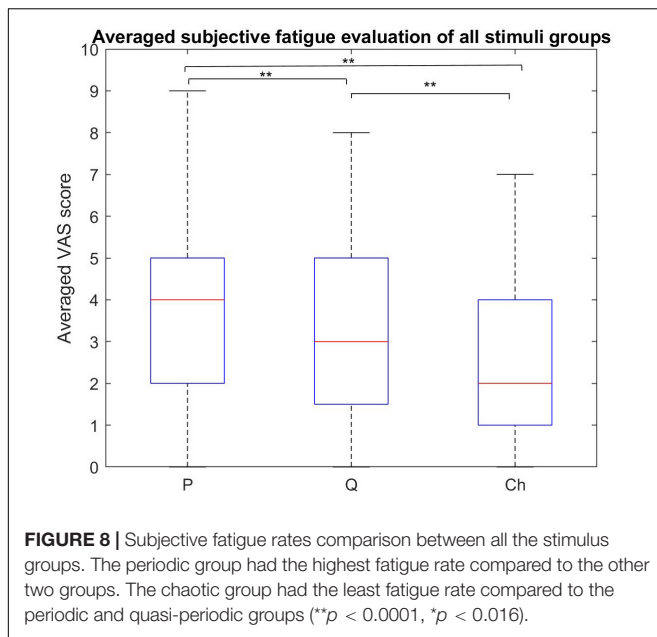
Details of the p -values for subjective fatigue comparisons using the Friedman test with Bonferroni correction are presented in Supplementary Table 1.

Between-Group Analysis of Subjective Visual Fatigue Rate

The Friedman test showed that the subjective visual fatigue scores differed across the three stimulus groups [$\chi^2(2) = 28.69$, $p = 0.0001$]. Participants reported higher subjective fatigue for the periodic stimuli compared to the quasi-periodic ($Z = 2.931$, $p = 0.003$) and chaotic stimuli ($Z = 4.429$, $p = 0.0001$). In addition, they also felt higher fatigue for the quasi-periodic stimuli compared to the chaotic group ($Z = 3.466$, $p = 0.001$).

DISCUSSION

In this study, for the first time, we used quasi-periodic and chaotic stimuli with different orthogonal characteristics and compared them with periodic stimuli commonly employed in SSVEP-based BCIs that use EEG data. We also compared the level of subjective



visual fatigue caused by these three stimuli on young adult participants. For this purpose, three groups of visual stimuli with different temporal dynamics (periodic, quasi-periodic, and chaotic) from simple sinusoidal frequencies to complex stimuli were generated from sine-circle and logistic maps and used for evoking visual potentials.

Periodic stimuli have been used for years in VEP generation for eliciting SSVEP responses that are known for their relatively high ITR, less training time (Parini et al., 2009), and practical BCI applications (Lalor et al., 2005; Muller-Putz and Pfurtscheller, 2008; Bin et al., 2009b; Yin et al., 2015; Lin et al., 2016; Wang Y.T. et al., 2017; Wang et al., 2018). Our results showed that the introduced dynamical visual stimuli (quasi-periodic and chaotic stimulus groups) could also evoke discriminative responses and can have even better target identification accuracies than the periodic visual stimulus group using the CCA method. In addition, compared to the other stimulus groups (periodic and quasi-periodic), the obtained accuracy values of target identification for the chaotic group by employing the CCA method for template generation approaches M1 (stimuli waveforms considered as a template) and M2 (templates generated from training EEG dataset) were the highest, with values of $M = 86.78\%$, $SE = 1.8\%$ and $M = 85.1\%$, $SE = 2.2\%$, respectively. The results of the M1 approach for the periodic, quasi-periodic, and chaotic stimuli indicate that their corresponding EEG responses correlated with their stimuli waveforms. It has been reported that the temporal structures of quasi-rhythmic stimuli are reflected in the brain responses in the visual cortex (Keitel et al., 2017).

Auto- and Cross-Correlation Function of Stimulus Groups

The stimuli in the chaotic and quasi-periodic groups as well as in the periodic group had orthogonal characteristics (Figure 3). This

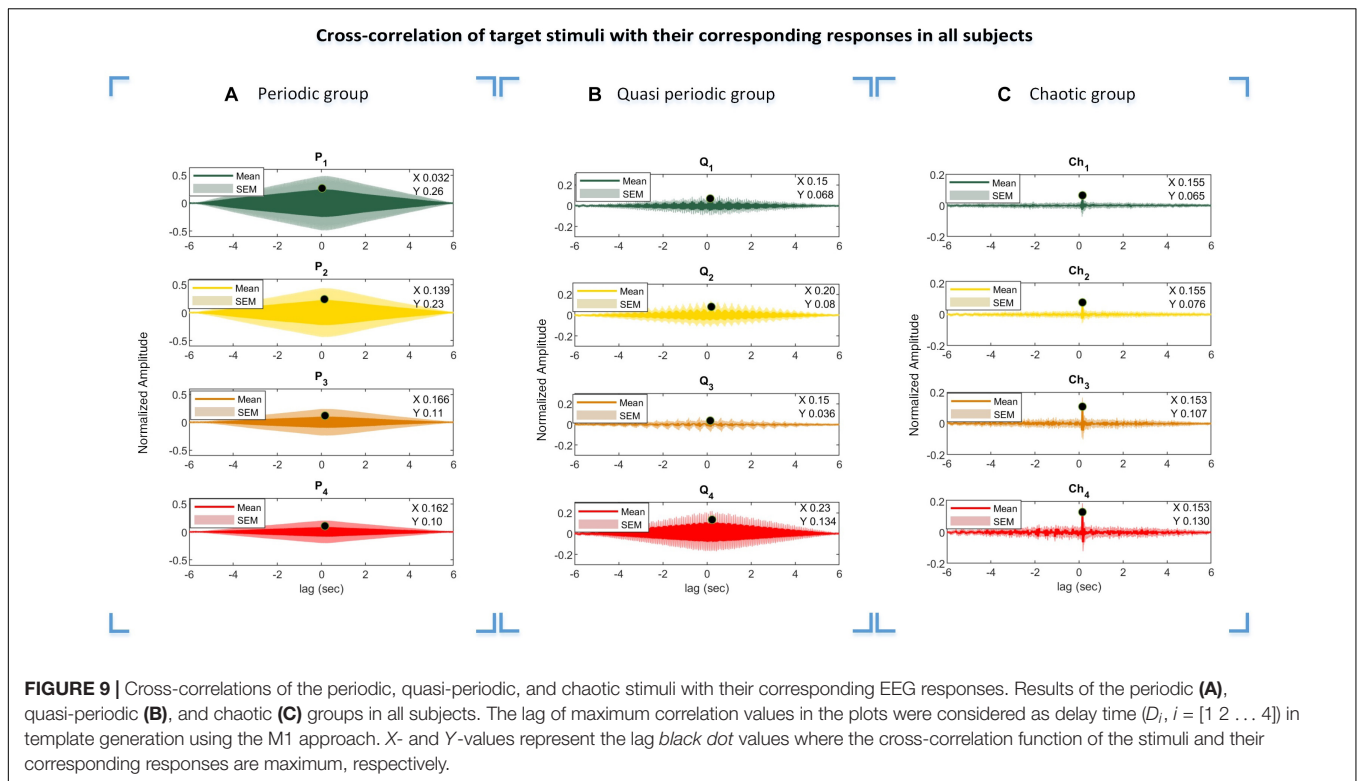
was demonstrated by the fact that the pairwise cross-correlation values between the stimuli were less than the auto-correlation values for the target stimuli (Figure 3). The cross-correlation functions showed that the stimuli within each stimulus group were not correlated because their cross-correlation values were close to zero. This meant that these stimuli were nearly orthogonal and the interference between the stimuli would be reduced in possible BCI applications. It is worth noting that the chaotic group's auto-correlation exhibited a Dirac-like function, meaning that while these stimuli were orthogonal, they did not correlate with themselves. This feature was absent in the periodic and quasi-periodic groups, which required a higher level of synchronization between the visual stimuli and their EEG responses. The concept of Dirac-like auto-correlation function has been used in code-modulated BCIs for generating uncorrelated target stimuli from one code by the process of shifting (Bin et al., 2011).

Cross-Correlation Function of Stimuli and Responses

The cross-correlation function of the presented stimuli and their corresponding responses suggest that the visual pathway system serves as an input and the evoked potentials as the system output. The lag of maximum of the cross-correlation function is considered as a system delay, which was used in our analysis especially in the CCA method for the M1 approach to generate templates from the presented stimuli. Due to the periodic and semi-periodic nature of the cross-correlation function (as seen in Figures 9A,B), compensating for the delay in templates was not necessary. However, compensating for the delay was vital for the chaotic group because the chaotic stimuli correlated with their corresponding responses in a specific time delay (Figure 9C). For the CCA method using template generation from the training dataset (M2 approach), the time delay compensation was not needed as the inherent time delay was embedded in the templates extracted from the training dataset.

Target Identification Results Comparison

The highest accuracy for the chaotic group was obtained by CCA using the M2 approach, while the lowest accuracy was obtained by the coherence method using the M2 approach. The much lower accuracy seen with the chaotic stimuli using coherence analysis may be explained by the fact that the spectra of these stimuli are highly similar, making them less discriminative compared to the other stimulus groups (periodic and quasi-periodic) (column 2 in Figure 2C). As the coherence analysis quantified the synchronization of the spectral information of two variables, for the periodic stimuli (single frequency) and even the quasi-periodic stimuli (containing multiple dominant frequencies), measuring the amount of synchronization between the narrow frequency bands (Vaid et al., 2015) was relatively less likely to be impacted by noise. However, as the chaotic stimulus spectra are similar and less discriminant (column 2 in Figure 2C) compared to the other stimulus groups, coherence analysis using the M2 approach is not recommended for chaotic stimuli. We suggest



the coherence method with the M1 approach for the analysis of chaotic stimuli.

While using the M1 templates with the coherence method led to a lower accuracy than with the CCA method, there is some benefit to using the coherence method with chaotic stimuli. Specifically, unlike CCA, coherence analysis is not sensitive to the time lag between variables (Guevara and Corsi-Cabrera, 1996). Therefore, using the coherence method could reduce the training time because it removes the need to obtain training data in order to extract the time lag needed for the time domain correlation.

The accuracy values of the M2 approach were found to be relatively higher compared to M1 in the CCA analysis for the quasi-periodic and chaotic stimuli (Figure 6 and Table 1). This means that the EEG response to the chaotic and quasi-periodic stimuli may contain not only the stimulus-locked components but also more complex dynamics that did not correlate with the visual stimuli while being discriminative.

Within-Group Subjective Visual Fatigue Rate Evaluation

From Figure 7, it can be seen that the mean VAS scores of the periodic stimulus group ($P_1 - P_4$, corresponding to frequencies of 20, 25, 35, and 40 Hz) decreased as the frequency of the target stimuli increased. These results confirm the fact that higher frequencies cause a less subjective visual fatigue level compared to lower ones (Allison et al., 2010; Volosyak et al., 2011; Yoshimoto et al., 2017). The statistical results show significant differences between all the pairs, except for $P_1 - P_2$ and $P_3 - P_4$ which were close to each other compared to the other pairs.

Q_4 stimulus had higher VAS scores compared to Q_1 . This may be due to the fact that Q_4 stimulus had dominant components in lower frequencies (column 2 in Figure 2B) compared to Q_1 , possibly leading to a more subjective visual fatigue. Ch_1 stimuli caused lower subjective visual fatigue compared to Ch_3 and Ch_4 . This could be due to the differences in the spectrum of Ch_1 compared to those of Ch_3 and Ch_4 (column 2 in Figure 2C) which tend to be in the higher frequencies.

In summary, the periodic stimulus group was less favorable considering the higher subjective visual fatigue level compared to the quasi-periodic and chaotic stimulus groups. For designing homogenous BCI, it is recommended to optimize the quasi-periodic and chaotic groups' orthogonal stimuli by evaluating their auto- and cross-correlation functions while at the same time choosing appropriate frequency bandwidths to minimize variations in the subjective visual fatigue.

Between-Group Subjective Fatigue Rate Evaluation

The comparison of the subjective visual fatigue rates of the periodic, quasi-periodic, and chaotic stimulus groups showed that the chaotic group caused less visual fatigue compared to the other two stimulus groups. The quasi-periodic group caused lower levels of visual fatigue compared to the periodic one (Figure 8). These results indicate the superiority of using the chaotic group for designing new comfortable and ergonomic VEP-based BCIs. Our recent study also showed that visual stimuli with chaotic characteristics lead to significantly less visual fatigue (Shirzhiyan et al., 2019).

The visual fatigue reduction seen in the chaotic and even the quasi-periodic stimuli group could be due to their dynamical and complex nature which is more compatible with the visual system compared to synthesized single frequencies. It has been shown that the periodic stimuli that exist in nature are not very pure in tone and have more than a single frequency as they contain quasi-rhythmic components and have a complex dynamical structure (Kayser et al., 2003; Butts et al., 2007; Mazzoni et al., 2011).

A simple deterministic dynamical system is also able to generate extremely unpredictable, divergent, and fractal behaviors (Boeing, 2016). These behaviors contain infinitely self-similar patterns avoiding exact repetition (periodicity). It is shown that fractal images and natural patterns are more appealing compared to the synthesized ones (Redies, 2007; Chapeau-Blondeau et al., 2009; Hagerhall et al., 2015; Kardan et al., 2015), and also the chaotic patterns with high fractal dimension and Lyapunov exponent are more aesthetically pleasing (Aks and Sprott, 1996). The application of natural visual stimuli that have sparse encoding can induce a resonant state leading to the adaptation of the visual system to natural patterns (Sekuler and Bennett, 2001; Redies, 2007) and possibly lower visual discomfort. The results of the current study show that visual fatigue scores are lower for quasi-periodic and chaotic stimuli compared to periodic stimuli having one frequency. It is speculated that this could be potentially because of the adaptation of the visual system to the presented complex dynamical stimuli.

Additionally, the chaotic, quasi-periodic, and periodic stimulus groups were closer to the $1/f$ amplitude spectrum, with the chaotic group being the nearest (dotted black line in the amplitude spectra plots of **Figure 2**). This pattern matches our results of the VAS scores as the chaotic group had the least visual fatigue in the same order with the other two groups. The relevance of a comparatively less visual fatigue and nearness of the chaotic stimuli to the $1/f$ amplitude spectrum is in agreement with previous studies reporting that the visual system encodes stimuli with $1/f$ amplitude spectral information (Tan and Yao, 2009; Ellemberg et al., 2012; Isherwood et al., 2017; Yoshimoto et al., 2017).

Limitations and Plans for Future Studies

Our study has several limitations. Within-group analysis of the subjective visual fatigue rates shows significant differences in all the three groups. In practice, it is not favorable that different target stimuli have different discomfort levels. To avoid possible within-group differences, the parameters of the stimulus-generated maps for each stimulus group could be selected in order to have similar stimulus spectra while at the same time preferring a higher frequency range instead of a lower one.

In this research, we did not study the optimization process for selecting the appropriate parameters of the quasi-periodic and chaotic stimuli. For future studies, optimization of the parameters with the aim of having a sharper and greater auto-correlation function of the target stimuli and a lower cross-correlation function with other stimuli should be considered. It is possible that such optimization can lead to better accuracy results.

The calculated lag times from the cross-correlation functions in three different stimulus groups represent interesting patterns.

As can be seen from **Figure 9**, the obtained delay for each target stimulus group differed from each other mainly in the periodic stimulus group, while this delay was almost constant among the target stimuli in the quasi-periodic and chaotic stimulus groups. The diversity in the delay lags could potentially be due to the non-linear behavior of the visual system to the presented input. We plan to investigate this effect in a future project and study the reasons leading to differential system delays for different stimulus characteristics.

In our previous study, we have shown that using binary chaotic codes *versus* m -sequences could decrease the subjective visual fatigue, and this could be used as a modulating code in c-VEP-based BCIs. Additionally, in this study, we found that the chaotic stimulus group provided very high discrimination between its individual stimuli, Ch_1 – Ch_4 , and could reduce the fatigue rate better when compared to the traditional stimuli for VEP generation (periodic stimuli). For further studies, it would be probably feasible to attempt using chaotic stimuli generated from other chaotic maps (such as Hanon map) and as short as codes commonly used in c-VEP studies. This could lead to the design of more comfortable and ergonomic c-VEP-based BCIs.

CONCLUSION

In this study, we introduced for the first time quasi-periodic and chaotic visual stimuli for evoking VEPs in order to use them in VEP-based BCIs and compared them with traditional periodic stimuli used in SSVEP-based studies. The presented complex stimuli (quasi-periodic and chaotic stimuli) satisfy the necessities for use as visual stimuli in VEP-based BCIs. The best target identification accuracy was obtained for the chaotic stimuli. Potentially due to the more natural-like characteristics of the chaotic and quasi-periodic stimuli, they led to less subjective visual fatigue compared to the periodic stimulus group.

DATA AVAILABILITY STATEMENT

All datasets generated for this study are included in the article/**Supplementary Material**.

ETHICS STATEMENT

The studies involving human participants were reviewed and approved by the office of research review board and the research ethics committee of the Tehran University of Medical Sciences with the LREC protocol number IR.TUMS.REC.1394.2110. The patients/participants provided their written informed consent to participate in this study.

AUTHOR CONTRIBUTIONS

ZS: data acquisition, analysis and interpretation, and first draft of manuscript. AK: data acquisition and analysis and contribution to manuscript writing. MF: hardware design and data acquisition. ES and MG: data acquisition and analysis. AM: study design,

hardware, data interpretation, and supervision. MH: data interpretation, design, overall supervision, and manuscript review. AJ: study design, funding, project supervision, and principal investigator. All authors contributed to the article and approved the submitted version.

FUNDING

This work was supported by Tehran University of Medical Sciences (grant no. 30946).

REFERENCES

- Aihara, K. (1989). Chaotic neural networks (Bifurcation phenomena in nonlinear systems and theory of dynamical systems). *Res. Instit. Math. Anal.* 710, 145–163.
- Aihara, K., Matsumoto, G., and Ikegaya, Y. (1984). Periodic and non-periodic responses of a periodically forced Hodgkin-Huxley oscillator. *J. Theoret. Biol.* 109, 249–269. doi: 10.1016/s0022-5193(84)80005-3
- Aitken, R. C. (1969). A growing edge of measurement of feelings [Abridged] measurement of feelings using visual analogue scales. *J. R. Soc. Med.* 62, 989–993.
- Ajami, S., Mahnam, A., and Abootalebi, V. (2018). Development of a practical high frequency brain-computer interface based on steady-state visual evoked potentials using a single channel of EEG. *Biocybernet. Biomed. Eng.* 38, 106–114. doi: 10.1016/j.bbe.2017.10.004
- Aks, D. J., and Sprott, J. C. (1996). Quantifying aesthetic preference for chaotic patterns. *Empir. Stud. Arts* 14, 1–16. doi: 10.2190/6v31-7m9r-t915-cdg9
- Allison, B., Luth, T., Valbuena, D., Teymourian, A., Volosyak, I., and Graser, A. (2010). BCI demographics: how many (and what kinds of) people can use an SSVEP BCI? *IEEE Trans. Neural Syst. Rehabil. Eng.* 18, 107–116. doi: 10.1109/tnsre.2009.2039495
- Allison, B. Z., McFarland, D. J., Schalk, G., Zheng, S. D., Jackson, M. M., and Wolpaw, J. R. (2008). Towards an independent brain-computer interface using steady state visual evoked potentials. *Clin. Neurophysiol.* 119, 399–408. doi: 10.1016/j.clinph.2007.09.121
- Aminaka, D., Makino, S., and Rutkowski, T. M. (2015). “Eeg filtering optimization for code-modulated chromatic visual evoked potential-based brain-computer interface,” in *Proceedings of the International Workshop on Symbiotic Interaction*, Berlin.
- Atick, J. J., and Redlich, A. N. (1992). What does the retina know about natural scenes? *Neural Comput.* 4, 196–210. doi: 10.1162/neco.1992.4.2.196
- Attinger, E., Anne, A., and McDonald, D. (1966). Use of fourier series for the analysis of biological systems. *Biophys. J.* 6:291. doi: 10.1016/s0006-3495(66)86657-2
- Bijur, P. E., Silver, W., and Gallagher, E. J. (2001). Reliability of the visual analog scale for measurement of acute pain. *Acad. Emerg. Med.* 8, 1153–1157. doi: 10.1111/j.1553-2712.2001.tb01132.x
- Bin, G., Gao, X., Wang, Y., Hong, B., and Gao, S. (2009a). VEP-based brain-computer interfaces: time, frequency, and code modulations [Research Frontier]. *IEEE Comput. Intellig. Magaz.* 4, 22–26. doi: 10.1109/mci.2009.934562
- Bin, G., Gao, X., Yan, Z., Hong, B., and Gao, S. (2009b). An online multi-channel SSVEP-based brain-computer interface using a canonical correlation analysis method. *J. Neural Eng.* 6:046002. doi: 10.1088/1741-2560/6/4/046002
- Bin, G., Gao, X., Wang, Y., Li, Y., Hong, B., and Gao, S. (2011). A high-speed BCI based on code modulation VEP. *J. Neural Eng.* 8:025015. doi: 10.1088/1741-2560/8/2/025015
- Blake, R., and Lee, S.-H. (2005). The role of temporal structure in human vision. *Behav. Cogn. Neurosci. Rev.* 4, 21–42. doi: 10.1177/1534582305276839
- Boeing, G. (2016). Visual analysis of nonlinear dynamical systems: chaos, fractals, self-similarity and the limits of prediction. *Systems* 4:37. doi: 10.3390/systems4040037
- Butts, D. A., Weng, C., Jin, J., Yeh, C.-I., Lesica, N. A., Alonso, J.-M., et al. (2007). Temporal precision in the neural code and the timescales of natural vision. *Nature* 449:92. doi: 10.1038/nature06105
- Camazine, S., Deneubourg, J.-L., Franks, N. R., Sneyd, J., Bonabeau, E., and Theraula, G. (2003). *Self-Organization in Biological Systems*. Princeton, NJ: Princeton University Press.
- Chang, M. H., Baek, H. J., Lee, S. M., and Park, K. S. (2014). An amplitude-modulated visual stimulation for reducing eye fatigue in SSVEP-based brain-computer interfaces. *Clin. Neurophysiol.* 125, 1380–1391. doi: 10.1016/j.clinph.2013.11.016
- Chapeau-Blondeau, F., Chauveau, J., Rousseau, D., and Richard, P. (2009). Fractal structure in the color distribution of natural images. *Chaos Solitons Fract.* 42, 472–482. doi: 10.1016/j.chaos.2009.01.008
- Chen, X., Wang, Y., Nakanishi, M., Gao, X., Jung, T.-P., and Gao, S. (2015). High-speed spelling with a noninvasive brain-computer interface. *Proc. Natl. Acad. Sci. U.S.A.* 112, E6058–E6067.
- Chien, Y.-Y., Lin, F.-C., Zao, J. K., Chou, C.-C., Huang, Y.-P., Kuo, H.-Y., et al. (2017). Polychromatic SSVEP stimuli with subtle flickering adapted to brain-display interactions. *J. Neural Eng.* 14:016018. doi: 10.1088/1741-2552/aa550d
- Choi, I. (2017). A *Sensorimotor Rhythm (SMR)-Based Brain-Computer Interface (BCI) Controlled Functional Electrical Stimulation (FES) for Restoration of Hand Grasping and Extension Functions*. Raleigh, CA: NC State University Libraries.
- Chumerin, N., Manyakov, N. V., van Vliet, M., Robben, A., Combaz, A., and Van Hulle, M. M. (2012). Steady-state visual evoked potential-based computer gaming on a consumer-grade EEG device. *IEEE Trans. Comput. Intellig. Games* 5, 100–110. doi: 10.1109/tciaig.2012.2225623
- Correa, A., and Nobre, A. C. (2008). Neural modulation by regularity and passage of time. *J. Neurophysiol.* 100, 1649–1655. doi: 10.1152/jn.90656.2008
- Costantino, R., Desharnais, R., Cushing, J., and Dennis, B. (1997). Chaotic dynamics in an insect population. *Science* 275, 389–391. doi: 10.1126/science.275.5298.389
- Crichton, N. (2001). Visual analogue scale (VAS). *J. Clin. Nurs.* 10:706.
- DeTommaso, M., Scirucchio, V., Guido, M., Sasanelli, G., and Puca, F. (1999). Steady-state visual-evoked potentials in headache: diagnostic value in migraine and tension-type headache patients. *Cephalalgia* 19, 23–26. doi: 10.1046/j.1468-2982.1999.1901023.x
- Elleberg, D., Hansen, B. C., and Johnson, A. (2012). The developing visual system is not optimally sensitive to the spatial statistics of natural images. *Vis. Res.* 67, 1–7.
- Essl, G. (2006). *Circle Maps as Simple Oscillators for Complex Behavior: I. Basics*. Available online at: <http://citeseerx.ist.psu.edu/viewdoc/download?doi=10.1.1.129.5143&rep=rep1&type=pdf> doi: 10.1016/j.visres.2012.06.018 (accessed January 2, 2020).
- Feng, P., Wu, Y., and Zhang, J. (2017). A Route to chaotic behavior of single neuron exposed to external electromagnetic radiation. *Front. Comput. Neurosci.* 11:94. doi: 10.3389/fncom.2017.00094
- Fisher, R. S., Harding, G., Erba, G., Barkley, G. L., and Wilkins, A. (2005). Photocopy and pattern-induced seizures: a review for the epilepsy foundation of america working group. *Epilepsia* 46, 1426–1441. doi: 10.1111/j.1528-1167.2005.31405.x
- Freeman, W. J. (1992). Tutorial on neurobiology: from single neurons to brain chaos. *Intern. J. Bifurc. Chaos* 2, 451–482. doi: 10.1142/s0218127492000653

ACKNOWLEDGMENTS

The authors would like to thank all subjects of this study for their cooperation.

SUPPLEMENTARY MATERIAL

The Supplementary Material for this article can be found online at: <https://www.frontiersin.org/articles/10.3389/fnins.2020.534619/full#supplementary-material>

- Gao, S., Wang, Y., Gao, X., and Hong, B. (2014). Visual and auditory brain-computer interfaces. *IEEE Trans. Biomed. Eng.* 61, 1436–1447. doi: 10.1109/tbme.2014.2300164
- Gift, A. G. (1989). Visual analogue scales: measurement of subjective phenomena. *Nurs. Res.* 38, 286–288.
- Grant, S., Aitchison, T., Henderson, E., Christie, J., Zare, S., Mc Murray, J., et al. (1999). A comparison of the reproducibility and the sensitivity to change of visual analogue scales, Borg scales, and Likert scales in normal subjects during submaximal exercise. *Chest* 116, 1208–1217. doi: 10.1378/chest.116.5.1208
- Guevara, M. A., and Corsi-Cabrera, M. (1996). EEG coherence or EEG correlation? *Intern. J. Psychophysiol.* 23, 145–153. doi: 10.1016/s0167-8760(96)00038-4
- Guger, C., Allison, B., and Edlinger, G. (2013). “State of the art in bci research: BCI award 2011,” in *Brain-Computer Interface Research*, ed. R. Fazel-Rezai (London: IntechOpen), 1–5. doi: 10.1007/978-3-642-36083-1_1
- Guo, F., Hong, B., Gao, X., and Gao, S. (2008). A brain-computer interface using motion-onset visual evoked potential. *J. Neural Eng.* 5:477. doi: 10.1088/1741-2560/5/4/011
- Gysels, E., and Celka, P. (2004). Phase synchronization for the recognition of mental tasks in a brain-computer interface. *IEEE Trans. Neural Syst. Rehabil. Eng.* 12, 406–415. doi: 10.1109/tnsre.2004.838443
- Haegens, S., and Golombic, E. Z. (2018). Rhythmic facilitation of sensory processing: a critical review. *Neurosci. Biobehav. Rev.* 86, 150–165. doi: 10.1016/j.neubiorev.2017.12.002
- Hagerhall, C. M., Laike, T., Kuller, M., Marcheschi, E., Boydston, C., and Taylor, R. (2015). Human physiological benefits of viewing nature: EEG responses to exact and statistical fractal patterns. *Nonlinear Dyn. Psychol. Life Sci.* 19, 1–12.
- Han, C., Xu, G., Xie, J., Chen, C., and Zhang, S. (2018). Highly interactive brain-computer interface based on flicker-free steady-state motion visual evoked potential. *Sci. Rep.* 8:5835.
- Hoebeek, F. E., Witter, L., Ruigrok, T. J., and De Zeeuw, C. I. (2010). Differential olivo-cerebellar cortical control of rebound activity in the *Cerebellar nuclei*. *Proc. Natl. Acad. Sci. U.S.A.* 107, 8410–8415. doi: 10.1073/pnas.0907118107
- Holz, E. M., Höhne, J., Staiger-Sälzer, P., Tangermann, M., and Kübler, A. (2013). Brain-computer interface controlled gaming: evaluation of usability by severely motor restricted end-users. *Artif. Intellig. Med.* 59, 111–120. doi: 10.1016/j.artmed.2013.08.001
- Hong, K.-S. (2011). Synchronization of coupled chaotic FitzHugh-Nagumo neurons via lyapunov functions. *Math. Comput. Simul.* 82, 590–603. doi: 10.1016/j.matcom.2011.10.005
- Isherwood, Z. J., Schira, M. M., and Spehar, B. (2017). The tuning of human visual cortex to variations in the $1/f_x$ amplitude spectra and fractal properties of synthetic noise images. *Neuroimage* 146, 642–657. doi: 10.1016/j.neuroimage.2016.10.013
- Ishikawa, T., Shimuta, M., and Häusser, M. (2015). Multimodal sensory integration in single cerebellar granule cells in vivo. *eLife* 4:e12916.
- Jiang, J., Yin, E., Wang, C., Xu, M., and Ming, D. (2018). Incorporation of dynamic stopping strategy into the high-speed SSVEP-based BCIs. *J. Neural Eng.* 15:046025. doi: 10.1088/1741-2552/aac605
- Jin, J., Sellers, E. W., Zhou, S., Zhang, Y., Wang, X., and Cichocki, A. (2005). A P300 brain-computer interface based on a modification of the mismatch negativity paradigm. *Intern. J. Neural Syst.* 25:1550011. doi: 10.1142/s0129065715500112
- Kapgate, D., and Kalbande, D. (2015). “A review on visual brain computer interface,” in *Advancements of Medical Electronics. Lecture Notes in Bioengineering*, eds S. Gupta, S. Bag, K. Ganguly, I. Sarkar, and P. Biswas (New Delhi: Springer), 193–206.
- Kardan, O., Demiralp, E., Hout, M. C., Hunter, M. R., Karimi, H., Hanayik, T., et al. (2015). Is the preference of natural versus man-made scenes driven by bottom-up processing of the visual features of nature? *Front. Psychol.* 6:471. doi: 10.3389/fncom.2017.00471
- Käthner, I., Wriessnegger, S. C., Müller-Putz, G. R., Kübler, A., and Halder, S. (2014). Effects of mental workload and fatigue on the P300, alpha and theta band power during operation of an ERP (P300) brain-computer interface. *Biol. Psychol.* 102, 118–129. doi: 10.1016/j.biopsycho.2014.07.014
- Kayser, C., Salazar, R. F., and Konig, P. (2003). Responses to natural scenes in cat V1. *J. Neurophysiol.* 90, 1910–1920. doi: 10.1152/jn.00195.2003
- Keihani, A., Shirzhiyan, Z., Farahi, M., Shamsi, E., Mahnam, A., Makkiabadi, B., et al. (2018). Use of sine shaped high-frequency rhythmic visual stimulus patterns for SSVEP response analysis and fatigue rate evaluation in normal subjects. *Front. Hum. Neurosci.* 12:201. doi: 10.3389/fnhum.2018.00201
- Keitel, C., Thut, G., and Gross, J. (2017). Visual cortex responses reflect temporal structure of continuous quasi-rhythmic sensory stimulation. *Neuroimage* 146, 58–70. doi: 10.1016/j.neuroimage.2016.11.043
- Klimek, L., Bergmann, K.-C., Biedermann, T., Bousquet, J., Hellings, P., Jung, K., et al. (2017). Visual analogue scales (VAS): measuring instruments for the documentation of symptoms and therapy monitoring in cases of allergic rhinitis in everyday health care. *Allergo J. Intern.* 26, 16–24. doi: 10.1007/s40629-016-0006-7
- Krusienski, D. J., McFarland, D. J., and Wolpaw, J. R. (2012). Value of amplitude, phase, and coherence features for a sensorimotor rhythm-based brain-computer interface. *Brain Res. Bull.* 87, 130–134. doi: 10.1016/j.brainresbull.2011.09.019
- La Rocca, D., Campisi, P., Vegso, B., Cserti, P., Kozmann, G., Babiloni, F., et al. (2014). Human brain distinctiveness based on EEG spectral coherence connectivity. *IEEE Trans. Biomed. Eng.* 61, 2406–2412. doi: 10.1109/tbme.2014.2317881
- Lachaux, J. P., Rodriguez, E., Martinerie, J., and Varela, F. J. (1999). Measuring phase synchrony in brain signals. *Hum. Brain Mapp.* 8, 194–208. doi: 10.1002/(sici)1097-0193(1999)8:4<194::aid-hbm4>3.0.co;2-c
- Lalor, E. C., Kelly, S. P., Finucane, C., Burke, R., Smith, R., Reilly, R. B., et al. (2005). Steady-state VEP-based brain-computer interface control in an immersive 3D gaming environment. *EURASIP J. Adv. Signal. Process.* 2005:706906.
- Lasley, D. J., and Cohn, T. (1981). Detection of a luminance increment: effect of temporal uncertainty. *JOSA* 71, 845–850. doi: 10.1364/josa.71.000845
- Lebedev, M. A., and Nicolelis, M. A. (2006). Brain-machine interfaces: past, present and future. *Trends Neurosci.* 29, 536–546. doi: 10.1016/j.tins.2006.07.004
- Lee, P.-L., Hsieh, J.-C., Wu, C.-H., Shyu, K.-K., Chen, S.-S., Yeh, T.-C., et al. (2006). The brain computer interface using flash visual evoked potential and independent component analysis. *Ann. Biomed. Eng.* 34, 1641–1654. doi: 10.1007/s10439-006-9175-8
- Lee, P.-L., Hsieh, J.-C., Shyu, K.-K., and Wu, Y.-T. (2008). Brain computer interface using flash onset and offset visual evoked potentials. *Clin. Neurophysiol.* 119, 605–616. doi: 10.1016/j.clinph.2007.11.013
- Lee, P.-L., Yeh, C.-L., Cheng, J. Y.-S., Yang, C.-Y., and Lan, G.-Y. (2011). An SSVEP-based BCI using high duty-cycle visual flicker. *IEEE Trans. Biomed. Eng.* 58, 3350–3359. doi: 10.1109/tbme.2011.2162586
- Liew, S.-H., Choo, Y.-H., Low, Y. F., and Yusoh, Z. I. M. (2015). Identifying visual evoked potential (VEP) electrodes setting for person authentication. *Int. J. Adv. Soft Comput. Appl.* 7, 85–99.
- Lin, K., Cinetto, A., Wang, Y., Chen, X., Gao, S., and Gao, X. (2016). An online hybrid BCI system based on SSVEP and EMG. *J. Neural Eng.* 13:026020. doi: 10.1088/1741-2560/13/2/026020
- Lin, Z., Zhang, C., Wu, W., and Gao, X. (2006). Frequency recognition based on canonical correlation analysis for SSVEP-based BCIs. *IEEE Trans. Biomed. Eng.* 53, 2610–2614. doi: 10.1109/tbme.2006.886577
- Liu, Y., Wei, Q., and Lu, Z. (2018). A multi-target brain-computer interface based on code modulated visual evoked potentials. *PLoS One* 13:e0202478. doi: 10.1371/journal.pone.0202478
- Llinás, R. R. (1988). The intrinsic electrophysiological properties of mammalian neurons: insights into central nervous system function. *Science* 242, 1654–1664.
- Lv, M., Wang, C., Ren, G., Ma, J., and Song, X. (2016). Model of electrical activity in a neuron under magnetic flow effect. *Nonlinear Dyn.* 85, 1479–1490. doi: 10.1007/s11071-016-2773-6
- Ma, J., and Tang, J. (2017). A review for dynamics in neuron and neuronal network. *Nonlinear Dyn.* 89, 1569–1578. doi: 10.1007/s11071-017-3565-3
- Martinez, P., Bakardjian, H., and Cichocki, A. (2007). Fully online multicommand brain-computer interface with visual neurofeedback using SSVEP paradigm. *Comput. Intellig. Neurosci.* 94561. doi: 10.1155/2007/94561
- May, R. M. (1976). Simple mathematical models with very complicated dynamics. *Nature* 261:459. doi: 10.1038/261459a0
- Mazzoni, A., Brunel, N., Cavallari, S., Logothetis, N. K., and Panzeri, S. (2011). Cortical dynamics during naturalistic sensory stimulations: experiments and models. *J. Physiol. Paris* 105, 2–15. doi: 10.1016/j.jphysparis.2011.07.014
- McCane, L. M., Heckman, S. M., McFarland, D. J., Townsend, G., Mak, J. N., Sellers, E. W., et al. (2015). P300-based brain-computer interface (BCI) event-related

- potentials (ERPs): people with amyotrophic lateral sclerosis (ALS) vs. age-matched controls. *Clin. Neurophysiol.* 126, 2124–2131. doi: 10.1016/j.clinph.2015.01.013
- Middendorff, M., McMillan, G., Calhoun, G., and Jones, K. S. (2000). Brain-computer interfaces based on the steady-state visual-evoked response. *IEEE Trans. Rehabil. Eng.* 8, 211–214. doi: 10.1109/86.847819
- Molina, R., Relaño, A., Retamosa, J., Muñoz, L., Faleiro, E., and Gómez, J. (2010). “Perspectives on 1/f noise in quantum chaos,” in *Proceedings of the Journal of Physics: Conference Series, Volume 239, XXXIII Symposium on Nuclear Physics 5–8 January 2010, Morelos*.
- Muller-Putz, G. R., and Pfurtscheller, G. (2008). Control of an electrical prosthesis with an SSVEP-based BCI. *IEEE Trans. Biomed. Eng.* 55, 361–364. doi: 10.1109/tbme.2007.897815
- Müller-Putz, G. R., Scherer, R., Brauneis, C., and Pfurtscheller, G. (2005). Steady-state visual evoked potential (SSVEP)-based communication: impact of harmonic frequency components. *J. Neural Eng.* 2:123.
- Nakanishi, M., Wang, Y., Wang, Y. T., Mitsukura, Y., and Jung, T. P. (2014). A high-speed brain speller using steady-state visual evoked potentials. *Intern. J. Neural Syst.* 24:1450019. doi: 10.1142/s0129065714500191
- Nobukawa, S., and Nishimura, H. (2016). Chaotic resonance in coupled inferior olive neurons with the Llinás approach neuron model. *Neural Comput.* 28, 2505–2532. doi: 10.1162/neco_a_00894
- Nunez, P. L., Srinivasan, R., Westdorp, A. F., Wijesinghe, R. S., Tucker, D. M., Silberstein, R. B., et al. (1997). EEG coherence: I: statistics, reference electrode, volume conduction, Laplacians, cortical imaging, and interpretation at multiple scales. *Electroencephalogr. Clin. Neurophysiol.* 103, 499–515.
- Obleser, J., Henry, M. J., and Lakatos, P. (2017). What do we talk about when we talk about rhythm? *PLoS Biol.* 15:e2002794. doi: 10.1371/journal.pbio.2002794
- Parini, S., Maggi, L., Turconi, A. C., and Andreoni, G. (2009). A robust and self-paced BCI system based on a four class SSVEP paradigm: algorithms and protocols for a high-transfer-rate direct brain communication. *Comput. Intellig. Neurosci.* 2009:864564.
- Paul-Dauphin, A., Guillemin, F., Virion, J.-M., and Briancçon, S. (1999). Bias and precision in visual analogue scales: a randomized controlled trial. *Am. J. Epidemiol.* 150, 1117–1127. doi: 10.1093/oxfordjournals.aje.a009937
- Petrov, V., Ouyang, Q., and Swinney, H. L. (1997). Resonant pattern formation in an chemical system. *Nature* 388:655. doi: 10.1038/41732
- Potapov, A., and Ali, M. (2000). Robust chaos in neural networks. *Phys. Lett. A* 277, 310–322.
- Redies, C. (2007). A universal model of esthetic perception based on the sensory coding of natural stimuli. *Spat. Vis.* 21, 97–117. doi: 10.1163/156856808782713780
- Relano, A., Gómez, J., Molina, R., Retamosa, J., and Faleiro, E. (2002). Quantum chaos and 1/f noise. *Phys. Rev. Lett.* 89:244102.
- Riechmann, H., Finke, A., and Ritter, H. (2016). Using a cVEP-based brain-computer interface to control a virtual agent. *IEEE Trans. Neural Syst. Rehabil. Eng.* 24, 692–699. doi: 10.1109/tnsre.2015.2490621
- Rössert, C., Dean, P., and Porrill, J. (2015). At the edge of chaos: how cerebellar granular layer network dynamics can provide the basis for temporal filters. *PLoS Comput. Biol.* 11:e1004515. doi: 10.1371/journal.pone.1004515
- Saha, T., and Galic, M. (2018). Self-organization across scales: from molecules to organisms. *Philos. Trans. R. Soc. B* 373:20170113. doi: 10.1098/rstb.2017.0113
- Sakurada, T., Kawase, T., Komatsu, T., and Kansaku, K. (2015). Use of high-frequency visual stimuli above the critical flicker frequency in a SSVEP-based BMI. *Clin. Neurophysiol.* 126, 1972–1978. doi: 10.1016/j.clinph.2014.12.010
- Sanei, S., and Chambers, J. A. (2007). *EEG Signal Processing*. New York, NY: Wiley.
- Sekuler, A. B., and Bennett, P. J. (2001). Visual neuroscience: resonating to natural images. *Curr. Biol.* 11, R733–R736.
- Shirzhiyan, Z., Keihani, A., Farahi, M., Shamsi, E., Golmohammadi, M., Mahnam, A., et al. (2019). Introducing chaotic codes for the modulation of code modulated visual evoked potentials (c-VEP) in normal adults for visual fatigue reduction. *PLoS One* 14:e0213197. doi: 10.1371/journal.pone.0213197
- Spüler, M. (2017). A high-speed brain-computer interface (BCI) using dry EEG electrodes. *PLoS One* 12:e0172400. doi: 10.1371/journal.pone.0172400
- Strogatz, S. H. (2018). *Nonlinear Dynamics and Chaos: with Applications to Physics, Biology, Chemistry, and Engineering*. Boca Raton, FL: CRC Press.
- Suzuki, Y., Lu, M., Ben-Jacob, E., and Onuchic, J. N. (2016). Periodic, quasi-periodic and chaotic dynamics in simple gene elements with time delays. *Sci. Rep.* 6:21037.
- Takano, K., Komatsu, T., Hata, N., Nakajima, Y., and Kansaku, K. (2009). Visual stimuli for the P300 brain-computer interface: a comparison of white/gray and green/blue flicker matrices. *Clin. Neurophysiol.* 120, 1562–1566. doi: 10.1016/j.clinph.2009.06.002
- Tan, Z., and Yao, H. (2009). The spatiotemporal frequency tuning of LGN receptive field facilitates neural discrimination of natural stimuli. *J. Neurosci.* 29, 11409–11416. doi: 10.1523/jneurosci.1268-09.2009
- Tseng, B. Y., Gajewski, B. J., and Kluding, P. M. (2010). Reliability, responsiveness, and validity of the visual analog fatigue scale to measure exertion fatigue in people with chronic stroke: a preliminary study. *Stroke Res. Treat.* 2010:412964.
- Vaid, S., Singh, P., and Kaur, C. (2015). “EEG signal analysis for BCI interface: a review,” in *Proceedings of the 2015 Fifth International Conference on Advanced Computing & Communication Technologies*, Haryana.
- Verwulgen, S., Lacko, D., Justine, H., Kustermans, S., Moons, S., Thys, F., et al. (2018). “Determining comfortable pressure ranges for wearable EEG headsets,” in *Proceedings of the International Conference on Applied Human Factors and Ergonomics*, Cham.
- Vialatte, F.-B., Maurice, M., Dauwels, J., and Cichocki, A. (2010). Steady-state visually evoked potentials: focus on essential paradigms and future perspectives. *Prog. Neurobiol.* 90, 418–438. doi: 10.1016/j.pneurobio.2009.11.005
- Volosyak, I., Valbuena, D., Luth, T., Malechka, T., and Graser, A. (2011). BCI demographics II: how many (and what kinds of) people can use a high-frequency SSVEP BCI? *IEEE Trans. Neural Syst. Rehabil. Eng.* 19, 232–239. doi: 10.1109/tnsre.2011.2121919
- Wang, Y., Wang, R., Gao, X., Hong, B., and Gao, S. (2006). A practical VEP-based brain-computer interface. *IEEE Trans. Neural Syst. Rehabil. Eng.* 14, 234–240. doi: 10.1109/tnsre.2006.875576
- Wang, Y.-T., Nakanishi, M., Wang, Y., Wei, C.-S., Cheng, C.-K., and Jung, T.-P. (2017). An online brain-computer interface based on SSVEPs measured from non-hair-bearing areas. *IEEE Trans. Neural Syst. Rehabil. Eng.* 25, 14–21. doi: 10.1109/tnsre.2016.2573819
- Wang, Y., Chen, X., Gao, X., and Gao, S. (2017). A benchmark dataset for SSVEP-based brain-computer interfaces. *IEEE Trans. Neural Syst. Rehabil. Eng.* 25, 1746–1752. doi: 10.1109/tnsre.2016.2627556
- Wang, Z., Yu, Y., Xu, M., Liu, Y., Yin, E., and Zhou, Z. (2018). Towards a Hybrid BCI gaming paradigm based on motor imagery and SSVEP. *Intern. J. Hum. Comput. Interact.* 35, 197–205. doi: 10.1080/10447318.2018.1445068
- Wei, Q., Feng, S., and Lu, Z. (2016). Stimulus specificity of brain-computer interfaces based on code modulation visual evoked potentials. *PLoS One* 11:e0156416. doi: 10.1371/journal.pone.0156416
- Wei, Q., Liu, Y., Gao, X., Wang, Y., Yang, C., Lu, Z., et al. (2018). A novel c-VEP BCI paradigm for increasing the number of stimulus targets based on grouping modulation with different codes. *IEEE Trans. Neural Syst. Rehabil. Eng.* 26, 1178–1187. doi: 10.1109/tnsre.2018.2837501
- Wolpaw, J. R., Birbaumer, N., McFarland, D. J., Pfurtscheller, G., and Vaughan, T. M. (2002). Brain-computer interfaces for communication and control. *Clin. Neurophysiol.* 113, 767–791.
- Won, D.-O., Hwang, H.-J., Dähne, S., Müller, K.-R., and Lee, S.-W. (2015). Effect of higher frequency on the classification of steady-state visual evoked potentials. *J. Neural Eng.* 13:016014. doi: 10.1088/1741-2560/13/1/016014
- Xie, J., Xu, G., Luo, A., Li, M., Zhang, S., Han, C., et al. (2017). The role of visual noise in influencing mental load and fatigue in a steady-state motion visual evoked potential-based brain-computer interface. *Sensors* 17:1873. doi: 10.3390/s17081873
- Xie, J., Xu, G., Wang, J., Li, M., Han, C., and Jia, Y. (2016). Effects of mental load and fatigue on steady-state evoked potential based brain computer interface tasks: a comparison of modulated flickering and motion-reversal based visual attention. *PLoS One* 11:e0163426. doi: 10.1371/journal.pone.0163426
- Xie, J., Xu, G., Wang, J., Zhang, F., and Zhang, Y. (2012). Steady-state motion visual evoked potentials produced by oscillating newton’s rings: implications for brain-computer interfaces. *PLoS One* 7:e39707. doi: 10.1371/journal.pone.039707

- Xie, J., Xu, G., Zhao, X., Li, M., Wang, J., Han, C., et al. (2018). Enhanced Plasticity of Human Evoked Potentials by Visual Noise During the Intervention of Steady-State Stimulation Based Brain-Computer Interface. *Front. Neurobot.* 12:82. doi: 10.3389/fnbot.2018.00082
- Yan, W., Xu, G., Li, M., Xie, J., Han, C., Zhang, S., et al. (2017). Steady-state motion visual evoked potential (SSMVEP) based on equal luminance colored enhancement. *PLoS One* 12:e0169642. doi: 10.1371/journal.pone.00169642
- Yin, E., Zhou, Z., Jiang, J., Yu, Y., and Hu, D. (2014). A dynamically optimized SSVEP brain-computer interface (BCI) speller. *IEEE Trans. Biomed. Eng.* 62, 1447–1456. doi: 10.1109/tbme.2014.2320948
- Yin, E., Zhou, Z., Jiang, J., Yu, Y., and Hu, D. (2015). A dynamically optimized SSVEP brain-computer interface (BCI) speller. *IEEE Trans. Biomed. Eng.* 62, 1447–1456.
- Yoshimoto, S., Garcia, J., Jiang, F., Wilkins, A. J., Takeuchi, T., and Webster, M. A. (2017). Visual discomfort and flicker. *Vis. Res.* 138, 18–28. doi: 10.1016/j.visres.2017.05.015
- Zhanabaev, Z. Z., Grevtseva, T. Y., and Kozhagulov, Y. (2016). Nonlinear characteristics of neural signals. *arXiv [Preprint]*. Available online at: <https://arxiv.org/abs/1610.01147#:~:text=We%20have%20shown%20that%20time,%20Dsimilarity%20and%20self%20affinity> (accessed January 13, 2020).
- Zhanabaev, Z. Z., and Kozhagulov, Y. T. (2013). A generic model for scale-invariant neural networks. *J. Neurosci. Neuroeng.* 2, 267–271. doi: 10.1166/jnsne.2013.1057
- Zhang, Y., Zhou, G., Jin, J., Wang, M., Wang, X., and Cichocki, A. (2013). L1-regularized multiway canonical correlation analysis for SSVEP-based BCI. *IEEE Trans. Neural Syst. Rehabil. Eng.* 21, 887–896. doi: 10.1109/tnsre.2013.2279680
- Zhang, Y., Zhou, G., Jin, J., Wang, X., and Cichocki, A. (2014). Frequency recognition in SSVEP-based BCI using multiset canonical correlation analysis. *Intern. J. Neural Syst.* 24:1450013. doi: 10.1142/s0129065714500130

Conflict of Interest: The authors declare that the research was conducted in the absence of any commercial or financial relationships that could be construed as a potential conflict of interest.

Copyright © 2020 Shirzhiyan, Keihani, Farahi, Shamsi, GolMohammadi, Mahnam, Haidari and Jafari. This is an open-access article distributed under the terms of the Creative Commons Attribution License (CC BY). The use, distribution or reproduction in other forums is permitted, provided the original author(s) and the copyright owner(s) are credited and that the original publication in this journal is cited, in accordance with accepted academic practice. No use, distribution or reproduction is permitted which does not comply with these terms.